**Tu-AM-Sym II-1**

## THE MOLECULAR BASIS OF VISUAL SIGNALING

*M. L. Applebury, L. Baxter, J. Johnston, T. Li, and K. Volpp, Visual Sciences Center, The University of Chicago, Chicago, IL 60637*

Visual triggering in photoreceptors has become a paradigm for the mechanisms of sensory transduction, as well as for hormone, neurotransmitter, and other modulatory ligand-induced receptor signaling pathways. In vertebrate photoreceptors, the molecular components are well defined and the sequence of events is explicit. The cascade of action involves light-activation of the signal receptor, catalysis of G-protein nucleotide exchange, and activation of the target enzyme cGMP phosphodiesterase. Light thus triggers a decrease in the second messenger cGMP which in turn results in the closing of cGMP-dependent ion channels and hyperpolarization of the cell. Each of the components has been biochemically isolated; each has been cloned to give structural information. The current objectives are to examine the interfaces between components of the pathway and to come to a better understanding of their structure/function relationships. We have given particular attention to the target enzyme and to comparing variants in rod and cone cells.

The cGMP phosphodiesterase in rods consists of two differing large subunits and two identical small subunits ($\alpha\beta\gamma_2$); in cones the protein is a homodimer ($\alpha'_2$) with its own distinct $\gamma$' subunits. The enzymes belong to the family of cyclic nucleotide phosphodiesterases, and in particular to a sub-family whose N-terminal domains form non-catalytic cyclic nucleotide binding sites and whose C-terminal domains form the catalytic site. The non-catalytic sites have weak homology to the cyclic nucleotide regulatory domains of cAMP and cGMP protein kinases, implicating a potential regulatory role. We are addressing the following queries: What is the role of non-catalytic cGMP sites? Do they modulate the G-protein activation? Why do the rod and cone enzymes differ? What are the important differences in structure and function? Is the activation of the phosphodiesterase unique to a photoreceptor signaling mechanism or does this enzyme serve as a model for understanding target enzyme activation in signaling pathways?

**Tu-AM-Sym II-2**

## GTP-BINDING PROTEINS, ADENYLYL CYCLASE, AND ION CHANNELS IN OLFACTORY SIGNAL TRANSDUCTION

R. R. Reed[1,3,4], H. A. Bakalyar[1,4], R. S. Dhallan[2,4] and K. -W. Yau[3,4], Depts of Molecular Biology and Genetics[1], Biomedical Engineering[2] and Neuroscience,[3] Howard Hughes Medical Laboratories[4], Johns Hopkins School of Medicine, Baltimore, MD. 21205

The vertebrate olfactory system is exquisitely adapted for the detection and recognition of small odorant molecules. The presence of odorant stimulated adenylyl cyclase and cyclic-nucleotide gated channels in olfactory cilia implicates an olfactory second messenger cascade analogous to that operating in the visual system. Previous biochemical studies suggest a role for a stimulatory GTP-binding protein and adenylyl cyclase in olfaction. We have identified a novel species, $G_{olf\alpha}$ that is highly homologous to $G_{s\alpha}$ (88% amino acid identity) and is, therefore likely to stimulate adenylyl cyclase. The $G_{olf\alpha}$ mRNA is expressed exclusively in olfactory tissue. Moreover, utilizing a neuron depletion technique, its expression appears to be confined to olfactory sensory neurons. With monospecific antisera to this novel G-protein, we have localized $G_{olf}$ protein to the cilia of the receptor neurons.

Recently, we have shown that the majority of the adenylyl cyclase activity in the olfactory epithelium resides within the receptor neurons. We have collaborated with Dr. Alfred Gilman's laboratory to isolate cDNA clones which encode three distinct forms of this enzyme. Expression of one of these forms is confined to olfactory neurons. The expression of these forms of adenylyl cyclase in a mammalian expression system has revealed distinct biochemical properties.

The conversion of the intracellular second messenger into an electrical response is achieved by a cyclic nucleotide-activated ion channel. A cDNA clone encoding this channel, analogous to one studied previously in the visual system, was identified by nucleotide homology to the rod photoreceptor channel. The $K_{1/2}$ for activation of this channel is ~40μM cAMP, compatible with its putative role in olfactory signaling.

The molecular cloning approaches described here support the notion that novel components of a second messenger cascade, $G_{olf}$ olfactory-specific adenylyl cyclase, and a cyclic nucleotide-activated ion channel couple to as yet unidentified receptors and mediate olfaction. The extension of these studies to other signal transduction systems will likely shed some light on the function of these molecular components.

**Tu-AM-Sym II-3**

## TRANSDUCTION MECHANISMS IN GUSTATORY RECEPTOR CELLS.

Sue C. Kinnamon, Department of Anatomy and Neurobiology, Colorado State University, Ft. Collins, CO 80523 and Rocky Mountain Taste and Smell Center, University of Colorado Health Sciences Center, Denver, CO 80262.

The sensation of taste is mediated by aggregations of specialized neuroepithelial cells called taste buds. Taste transduction is initiated when taste stimuli interact with sites on the apical microvilli of taste receptor cells; the interaction produces a depolarizing receptor potential or action potential, leading to transmitter release and activation of gustatory afferent neurons. The mechanisms involved in the interaction of the taste stimulus with the receptor membrane are beginning to be understood, due to the application of patch-clamp and optical recording techniques to isolated taste receptor cells. What is emerging from these studies is that taste transduction, unlike other sensory modalities, cannot be explained by a single mechanism. In many species, $Na^+$ salt is transduced into receptor potentials by amiloride-sensitive $Na^+$ channels located on the apical membrane; the $Na^+$ simply passes through the channels to depolarize the cells. Sour taste, mediated by protons, utilizes apically-restricted, voltage-dependent $K^+$ channels in Necturus. The protons directly block the channels, producing a depolarizing receptor potential. There is evidence for the involvement of specific membrane receptors coupled to G-proteins and second messenger systems for sweet and some bitter stimuli. Sweet-tasting compounds are thought to activate adenylate cyclase, causing cAMP-dependent phosphorylation and closure of $K^+$ channels. The extremely bitter stimulus denatonium causes release of $Ca^{++}$ from intracellular stores, possibly by activation of inositol triphosphate. The elevated intracellular $Ca^{++}$ is thought to enhance transmitter release without changing the membrane potential of the taste cells. Thus, taste cells appear to utilize a variety of mechanisms, related in part to the diverse nature of the different taste modalities.

**Tu-AM-Sym II-4**

## THE INITIAL EVENTS IN HEARING AND EQUILIBRIUM: MECHANOELECTRICAL TRANSDUCTION BY HAIR CELLS OF THE INTERNAL EAR.

*A. J. Hudspeth, Department of Cell Biology and Neuroscience, University of Texas Southwestern Medical Center, Dallas, TX 75235.*

The sensory receptor in auditory, vestibular, and lateral-line organs is the hair cell. This epithelial cell responds electrically when mechanical stimuli deflect its hair bundle, which is a cluster of 20-300 elongated, microvillus-like processes extending from the apical cellular surface. By addressing three experimental questions, we are attempting to learn how stimulation gates the ion channels involved in mechanoelectrical transduction.

Where are the molecules responsible for mechanoelectrical transduction? Although earlier electrical experiments implied that transduction current enters channels at a hair bundle's distal tip, the study of fura-2 signals from $Ca^{2+}$ flowing through the channels has recently suggested that transduction occurs at the bundle's base. Our current experiments support the initial result: iontophoretic application of aminoglycoside antibiotics blocks transduction only when directed at the bundle's tip, not when focussed upon the bundle's basal insertion.

What are the molecules responsible for transduction? In a new, single-step procedure, we can embed hair bundles in an agarose gel, then isolate them by shearing the gel with respect to the hair-cell somata. In conjunction with sensitive, chemiluminescence-based techniques for protein detection, this "twist-off" procedure allows us to characterize numerous proteins in hair bundles. In addition to molecules known to contribute to the bundle's cytoskeleton, we observe several novel proteins that may be involved in the bundle's surface coat, in the transduction process, and in adaptation to maintained stimuli.

How are transduction channels gated by mechanical stimuli? The short latency of the hair cell's electrical response – as little as a few microseconds – suggests that forces applied to the hair bundle act directly to open transduction channels. Consistent with this view, measurements of a bundle's mechanical properties demonstrate a decrease in stiffness over the range of bundle positions in which transduction channels are opening and closing. This gating compliance is an analog of the capacitance associated with electrical gating of voltage-sensitive ion channels.

This research was supported by NIH grants DC00241 and DC00317.

**Tu-AM-G1**

ANALYSIS OF CHARGE MUTATIONS IN THE S4 REGION OF THE DELAYED RECTIFIER K CHANNEL RCK1. D. E. Logothetis, E. R. Liman, F. Weaver, S. Movahedi, C. Sattler, G. Koren, B. Nadal Ginard, P. Hess. Harvard Medical School.

The S4 region in voltage dependent ion channels is believed to form the sensor for voltage dependent channel gating. We have assessed the relative importance of S4 positively charged residues in RCK1 channels expressed in frog oocytes. We estimated the total gating valence ($z=RT/F*\ln P_o/V$) from the limiting slope of the log $P_o$ vs. voltage plot of steady-state activation, measured using a tail protocol with Rb as charge carrier and 550 ms depolarizations. In wildtype (WT) channels $z=7.6\pm.3e$ and 10% maximal activation ($P_{0.1}$) occurred at $-61\pm4$ mV. The mean results of the mutational analysis appear on Table 1.

| Mutant | WT | R1K | R1Q | R1N | R1E | R2K | R2Q | R2D | R3K | K7Q | K7E |
|---|---|---|---|---|---|---|---|---|---|---|---|
| z (e) | 7.6 | 5.2 | 2.9 | 4.1 | 2.1 | 5.3 | 6.2 | 3.7 | 7.5 | 8.2 | 6.4 |
| $P_{0.1}$(mV) | -61 | -37 | -45 | -92 | -37 | -51 | -100 | -135 | -66 | -52 | -32 |

R1: Arg292; R2: Arg295; R3: Arg298; K7: Lys307

With the exception of R3K we have not been able to obtain functional expression with mutations at R3, R4 (Arg 301), K5 (Lys 304), and R6 (Arg 307). The side-chain specific values of z and $P_{0.1}$ at R1, which differed even between residues of equal charge, imply that in addition to electrostatic forces, strong chemical interactions govern the thermodynamic stability of that residue. Mutations at this position must affect the movement of the remaining gating charge, since some of the observed changes in z are too large to be caused by the change of that charge alone. R2 mutations showed electrostatic interactions at that residue but since the changes in z between WT, R2Q and R2D were not additive, side-chain specific chemical interactions must occur at this residue too, as illustrated also by the change in z of R2K. In contrast R3K gave a WT phenotype. The K7 results are consistent with the view that K7 crosses only a small part of the applied field during activation, but its charge, located most closely to the channel's inner surface, changes the potential felt by the other intramembrane charges. Our results confirm S4 as a major voltage sensor, but show that individual charges make quantitatively very different contributions to the overall gating valence. R1 and R2 must be well isolated from the ion conduction pathway, since the unitary conductance was WT for mutants R1N, R1E, and R2D.

**Tu-AM-G2**

**HIGH TIME-RESOLUTION RECORDINGS FROM OOCYTES INJECTED WITH WILD-TYPE AND V1 MUTANT *SHAKER* 29-4 cDNAs**, Nathan E. Schoppa,# Ken McCormack,* Mark A. Tanouye* and Fred J. Sigworth,# #Dept. of Cellular and Molecular Physiology, Yale University School of Medicine, New Haven CT 06510, *Division of Biology, California Institute of Technology, Pasadena, CA 91125.

Mutating the first leucine in the conserved leucine heptad repeat region of *Shaker* cDNA 29-4 to valine causes a large depolarizing shift and a dramatic reduction in voltage sensitivity of channel activation. In search of an explanation for these changes, we recorded 'macroscopic' currents in membrane patches of oocytes injected with wild-type and V1 mutants. Recordings were made in the cell-attached mode with a depolarizing bath solution and frog Ringer solution in the pipette. Upon stepping to depolarized potentials from -80 mV, wild-type currents (A) begin to activate after a substantial delay. Mutant currents (B) have similarly large delays. The long delays would not be expected if the mutation produced a strong negative cooperativity among the subunits. Another interesting finding is that the wild-type channel appears to activate at an increasingly faster rate at potentials well beyond +50 mV.

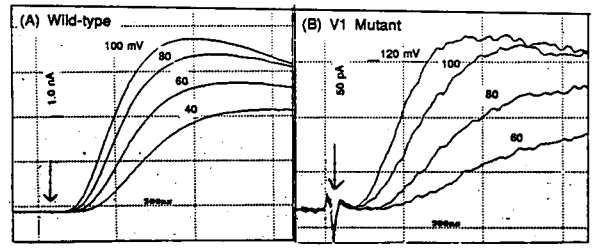


**Tu-AM-G3**

THE *DROSOPHILA eag* LOCUS ENCODES A NOVEL TYPE OF POTASSIUM CHANNEL SUBUNIT

Jeffrey W. Warmke, Rachel Drysdale and Barry Ganetzky
(Intro. by Chun-Fang Wu)
Laboratory of Genetics, University of Wisconsin,
Madison, Wisconsin 53706

The *ether `a-go-go* (*eag*) mutation in *Drosophila* confers repetitive firing of action potentials in motor axons and abnormal release of transmitter at the larval neuromuscular junction (Ganetzky and Wu, *Trends Neurosci.* **8:** 322, 1985). Measurements of potassium currents in larval muscles and cultured nerve cells using voltage-clamp and patch-clamp methodology have provided direct evidence for the reduction of one or more potassium currents ($I_K$ and $I_A$) in these cells (Wu *et al.*, *Science* **220:** 1077, 1983; Wu and Ganetzky, *Biophys. J.* **45:** 77, 1984; Sun and Wu, *Soc. Neurosci. Abstr.* **11:** 787, 1985). Therefore, it was proposed that *eag* encodes a component common to different types of potassium channels or plays a role in modulating the activity of these channels (Ganetzky and Wu, *Ann. Rev. Genet* **20:** 13, 1986).

To identify the product of the *eag* locus and define the role it plays in membrane excitability, we isolated genomic and cDNA clones from the *eag* locus (Drysdale *et al.*, Genetics, in press). This analysis revealed that the *eag* locus encodes a 10kb mRNA that is expressed predominantly in the heads of adults flies. Sequence analysis indicates that the *eag* locus encodes a 1174 amino acid protein containing seven putative membrane spanning domains characteristic of voltage sensitive potassium channels. The fourth hydrophobic domain has striking similarity to the S4 segment of other voltage sensitive ion channels. In addition, the fifth and sixth hydrophobic domains have significant similarity to the corresponding domains (H4 and H5) in the *Shaker* superfamily of potassium channel proteins. However, the other hydrophobic domains show little primary sequence similarity to the corresponding domains in the *Shaker* superfamily of potassium channel proteins. On the basis of these sequence comparisons and the results of electrophysiological analyses of *eag* mutants, we conclude that *eag* encodes a previously unidentified structural component of voltage sensitive potassium channels.

**Tu-AM-G4**

THE DROSOPHILA *slowpoke* GENE ENCODES A PUTATIVE STRUCTURAL COMPONENT OF A CALCIUM-ACTIVATED POTASSIUM CHANNEL.

Gail A. Robertson, Nigel S. Atkinson and Barry Ganetzky
(Intro. by Meyer Jackson), Laboratory of Genetics,
University of Wisconsin, Madison, WI 53706.

Calcium-activated potassium channels are not as well understood as their voltage-gated counterparts due to the lack of structural information available for this family of ion channels. We have used a molecular genetic approach to identify a gene affecting the function of calcium-activated potassium channels and to determine the primary structure of its encoded product. Mutations in the *slowpoke* (*slo*) locus of Drosophila eliminate a fast, calcium-activated potassium current in muscle and neurons[1,2]. We previously reported the cytological localization of the *slo* locus at 96A17 on the polytene chromosomes and the isolation of genomic DNA from this region[3]. Northern blot analysis and characterization of cDNA clones indicate that *slo* encodes a family of transcripts ranging from 5.8 to 10kb in size[4].

We have sequenced *slo* cDNA and find that it predicts a polypeptide with an S4-like region homologous to other ion channels. In addition, there is a region sharing a high degree of amino acid similarity with the H5 region of voltage-gated potassium channel polypeptides. In Shaker potassium channels, this domain has been proposed to participate in charybdotoxin binding[5] and ion permeation[6]. The effect of *slo* mutations on calcium-activated potassium currents, together with these sequence similarities, provide compelling evidence that *slo* encodes a structural component of calcium-activated potassium channels.

1. Elkins, Ganetzky and Wu, PNAS 83:8415 (1986); 2. Saito and Wu, Soc. Neurosci. Abst. 16:670 (1990); 3. Atkinson, Robertson and Ganetzky, ibid. 15:541 (1989); 4. Robertson, Atkinson and Ganetzky, ibid. 16:670 (1990); 5. MacKinnon and Miller, Science 245:1382 (1989); 6. Yool and Schwarz, Soc. Neurosci. Abst. 16:4 (1990). Supported by postdoctoral fellowships from NIH (GAR), MDA (NSA) and by grants from the NIH, Markey Foundation and a Klingenstein fellowship (BG).

Tu-AM-G5

**The Effect Of Mutations On The Kinetics Of CTX-Lq2 Block Of Shaker $K^+$ Channels.** Michael J. Root and Roderick MacKinnon. Department of Cellular and Molecular Physiology, Harvard Medical School.

Charybdotoxin (CTX) and several of its homologs inhibit Shaker $K^+$ channels in oocytes. Amino acids that are near the toxin binding site on the channel have been identified. Site-directed mutations involving some of these residues influence the inhibition constant ($K_i$) for toxin block by a simple through-space electrostatic interaction. In this study we ask how do such mutations influence the kinetics of the toxin interaction? To address this question we used the CTX homolog Lq-2 because it blocks the channel ($K_i$ = 12 nM) with rapid kinetics that can be easily measured. For convenience, we modified the Shaker $K^+$ channel with a mutation near the N-terminus that removes inactivation but does not alter toxin inhibition. Potassium currents of 100 - 2000 pA were typically observed in outside-out macropatches obtained from oocytes expressing the channel. Patches were placed in a rapid perfusion chamber in which solution could be changed in less than 1 second. The toxin concentration was abruptly changed and the association rate constant ($k_{on}$) and dissociation rate constant ($k_{off}$) were determined from the relaxation to equilibrium block. As expected for a simple bimolecular reaction, $k_{on}$ is linearly proportional to, and $k_{off}$ is independent of toxin concentration. The mutation E422K, known to increase $K_i$ (12 → 20 nM) by an electrostatic mechanism, decreases the association rate but has no effect on the rate of dissociation. These data indicate that mutations which electrostatically affect the bound state energy also affect the activation energy of binding by an equal amount.

Tu-AM-G6

**SITE-DIRECTED CHANGES IN A VOLTAGE-DEPENDENT $K^+$ CHANNEL ALTER IONIC SELECTIVITY AND OPEN-CHANNEL BLOCK.** Steven A. N. Goldstein and Christopher Miller, Howard Hughes Medical Institute, Graduate Department of Biochemistry, Brandeis University, Waltham, MA

We are studying a gene responsible for a slowly-activating, voltage-dependent, potassium-selective ion conductance. The gene was originally cloned from rat kidney mRNA and encodes a protein of only 130 amino acids with a single potential membrane-spanning $\alpha$-helical domain. In contrast, those $K^+$ channels which have previously been described at the molecular level are 5 times larger and appear to have at least 6 transmembrane regions. If the protein encoded by this gene is a channel, its molecular structure is unprecedented. This raises the question: Is this protein a channel or perhaps a "regulator" of channels normally silent in the expression system used here? We undertook to address this issue using a synthetic gene designed to facilitate cassette mutagenesis.

The ionic selectivity and voltage-dependent blockade of currents expressed in Xenopus oocytes injected with mRNA derived from either wild-type (w.t.) or mutants of this gene were studied by two-electrode voltage clamp. Selectivity among monovalent cations by the w.t. channel, as assessed by bi-ionic tail current reversal potentials, is characteristic of known $K^+$ channels: $K^+ > Rb^+ > NH_4^+ > Cs^+ > > Na^+ > Li^+$. Ionic blockade by $Ba^{2+}$ ($K_d$=2.5mM, $z\delta$=1.6) and $Cs^+$ ($K_d$=15mM, $z\delta$=0.3) was also classically behaved for w.t. Site-directed mutations within the putative membrane-spanning region have identified amino acid residues specifically affecting $Cs^+$ blockade and permeation. Changes at position 55 both diminish $Cs^+$ blocking affinity (mutant F55T, $K_d$=75mM, $z\delta$=0.8) and enhance $Cs^+$ permeability ($P_{K^+}/P_{Cs^+}$(w.t.)=16.7; $P_{K^+}/P_{Cs^+}$(F55T)=4.5) without affecting $Ba^{2+}$ blockade or permeability relative to $K^+$ of other monovalent cations.

These results strongly suggest that: i) this is a structural gene for a $K^+$ channel protein; ii) both a "selectivity filter" and a $Cs^+$ blocking site are influenced by position 55; and iii) a $Cs^+$ blocking site is within the conduction pathway. The combination of voltage-dependent, ion-selective channel function and structural brevity prompts us to suggest this minimal $K^+$ channel now be named "minK$^+$".

Tu-AM-G7

**High-level Expression of Charybdotoxin in E. coli.** Chul-Seung Park and Christopher Miller. HHMI, Graduate Dept. of Biochemistry, Brandeis Univ., Waltham, MA.

A synthetic gene was constructed for the purpose of producing milligram quantities of charybdotoxin (CTX), a 37-residue peptide that blocks the pore of several types of $K^+$ channels. A cleavable fusion protein containing the CTX coding sequence following the gene-9 protein of phage T7 was designed; a linker coding for Ile-Glu-Gly-Arg, the recognition site for a "restriction protease, "Factor Xa, was inserted immediately before the CTX sequence. The fusion protein was produced at high levels in E. coli (30-50 mg/L), and CTX, which accounts for about 10% of the mass of the fusion protein, was released after cleavage by factor Xa. The CTX peptide was purified and was converted to the active conformation by two post-translational modifications in vitro: (1) cyclization of the N-terminal glutamine to form pyroglutamate, and (2) formation of the 3 disulfide bonds. Disulfide bonds formed rapidly and with virtually 100% fidelity to those found in the native conformation of CTX. The recombinant CTX was quantitatively identical to native scorpion venom CTX in its block of single $Ca^{2+}$-activated $K^+$ channels and its NMR spectrum. Uncyclized CTX, with a free N-terminal glutamine, was a poor channel-blocker, with an off-rate about 5-fold faster than fully processed CTX.

This synthetic gene allows the production of specifically altered CTX for a detailed structure-function study of the interaction of this peptide with its receptor in the $K^+$ channel's externally facing mouth. Initially, we wish to know which of the 8 positively charged residues directly influence channel block. Replacement of Arg19 (located at one extreme end of the ellipsoidal molecule) by Gln has only minimal effects on the blocking kinetics. In contrast, substitution of Lys27 (located at the ellipsoid's midriff) by Gln lowers blocking affinity 100-fold, largely via an increased off-rate).

Tu-AM-G8

TOWARDS AN UNDERSTANDING OF THE MOLECULAR COMPOSITION OF K+ CHANNELS: PRODUCTS OF AT LEAST NINE DISTINCT SHAKER FAMILY K+ CHANNEL GENES ARE EXPRESSED IN A SINGLE CELL. Vega-Saenz de Miera, E., Chiu, N., Sen, K., Lau, D., Lin, J.W. and Rudy, B. Depts of Physiology & Biophysics and Biochemistry, New York University Medical Center, New York, NY 100116. (Introduced by: Felice Aull)

A large number of genes evolutionary related to the Shaker gene in Drosophila (the Shaker family) have been recently identified in mammals. These genes encode K+ channel subunits: cRNA synthesized from cloned cDNAs expressed voltage-dependent channels in Xenopus oocytes. It is likely that these channels are homomultimers, perhaps tetramers of the products of the cRNAs. Based on sequence similarity and hence evolutionary relatedness these genes are grouped into four subfamilies or classes. Class I are genes most similar to the Shaker gene, Class II to the Shab gene, Class III to the Shaw gene and Class IV to the Shal gene in Drosophila. The presence of a large number of K+ channel proteins are partly responsible for the large functional diversity of K+ channels. In addition, products of at least Class I genes can form heteromultimeric channels with novel functional properties. Heteromultimer formation, interactions with other types of subunits and postranslational modifications are also likely to contribute to K+ channel diversity. In order to understand the molecular composition of K+ channels in cells, the functional role of different Shaker (Sh) family subunits and the contribution of the various molecular mechanisms mentioned above to K+ channel diversity we have identified the Sh family genes expressed in PC12 cells. Single stranded cDNA synthesized from PC12 cell's mRNA and specific primers were used in a Polymerase Chain Reaction (PCR) to amplify DNA fragments corresponding to the four classes of Sh family genes. Three members of Class I (RCK1, RCK3 and RCK5); a member of class II (DRK1); three members of class III (NGK2, and two new members RKShIIIC and RKShIIID); and two new members of class IV (RKShIVA and RKShIVB) were thus identified. PC12 cell cDNA libraries were screened with the amplified fragments to obtain full sequences of the novel genes. The currents expressed by the products of these genes in Xenopus oocytes are compared to the currents recorded in PC12 cells. Support by NIH Grant: GM26976 to BR.

**Tu-AM-G9**

## A MINIMUM SEQUENCE FOR A FUNCTIONING DELAYED RECTIFYING $K^+$ CHANNEL (DRK1)

J.A. Drewe, M. Taglialatela, G.E. Kirsch, H.A. Hartmann, A.M. Brown and R.H. Joho. Departments of Molecular Physiology and Biophysics and Anesthesiology, Baylor College of Medicine, Houston, TX 77030.

Voltage-dependent ion channels consist of repeats having six transmembrane regions (S1-S6), flanked by cytoplasmic domains. We have been investigating the functional importance of the N- and C- termini for a delayed rectifier $K^+$ channel, DRK1 (Frech et al., Nature, 340:642). Removal of either 139 amino acids from the N-terminus or 318 amino acids from the C-terminus maintained $K^+$ channel function while altering activation, deactivation and inactivation kinetics (VanDongen et al., Neuron, in press). Further deletions in the C-terminus were engineered by taking advantage of natural restriction enzyme sites (C351), exonuclease (C422), and utilizing engineered silent restriction sites (C448 and C486). cRNAs from linearized transcripts were injected into Xenopus oocytes at 2-10 ng per egg. The C486 construct ending in the linker region between S5 and S6 and C448 at the end of S6 did not express voltage dependent $K^+$ channels. The C351 and C422 constructs expressed to functional $K^+$ channels. Therefore, a core region that includes the six transmembrane segments and a 25 amino acid section 3' to the sixth transmembrane region are necessary and sufficient for the formation of channels with the properties of a delayed rectifying $K^+$ channel. We are in the process of defining the limits at the N-terminus for channel function. These deletion constructs will be helpful in defining the influence of the cytoplasmic termini on $K^+$ channel function. Supported by NIH NS23877 and NS28407.

Tu-AM-H1

COEXISTENCE OF INOSITOL 1,4,5-TRISPHOSPHATE-GATED AND CALCIUM-GATED CHANNELS IN CEREBELLUM: DIFFERENCES IN CALCIUM SENSITIVITY. I. Bezprozvanny, B.E. Ehrlich, F. Mkparu, J. Watras. Depts. of Med. and Physiol., Univ. of CT, Farmington, CT 06030 (Intro. by L.B. Cohen)

Calcium (Ca) release from intracellular stores has been shown to occur by two types of Ca release channels. When binding assays were done using endoplasmic reticulum vesicles isolated from canine cerebellum both inositol 1,4,5-trisphosphate ($InsP_3$) and ryanodine binding sites were found. When the same vesicles were incorporated into planar bilayers two types of ligand-gated Ca channels were observed with characteristics corresponding to the receptors identified in binding assays. The first channel type was activated by addition of 0.1-2 uM $InsP_3$ and had four conductance levels in multiples of 20 pS. Adenine nucleotides increased the open probability when $InsP_3$ was present, but not in the absence of $InsP_3$. The second channel type was seen after addition of 330 uM AMP-PCP without $InsP_3$ present, had a conductance of 45 pS (sub levels were also observed), and was kinetically distinct from the $InsP_3$-gated channels. Also, the second channel type was inhibited completely by 2 uM ruthenium red, whereas the $InsP_3$ channel was unaffected by 10 uM ruthenium red. The Ca-dependence of the two channel types differed. The $InsP_3$-gated channel showed a biphasic dependence of Ca in the physiological range of cytoplasmic Ca with maximum activity observed at about 0.2 uM free Ca and a sharp decrease in activity on either side of the maximum. The Ca-dependence for the second type of channel also was biphasic, with maximum activity maintained between 1 and 100 uM Ca. The Ca-dependence for the second channel type could be fit assuming a single activating site and a single inhibitory site. In contrast, to fit the Ca-dependence of the $InsP_3$-gated channel we had to assume either cooperative activating and inhibitory sites each with Hill coefficients of two or four independent activating and four independent inhibitory sites. Supported by NIH grant HL-33026.

Tu-AM-H2

HIGH CONCENTRATIONS OF CALCIUM AND ATP REDUCE THE OPEN PROBABILITY OF THE SHEEP CARDIAC SARCOPLASMIC RETICULUM CALCIUM-RELEASE CHANNEL.

R. Sitsapesan, A. Boraso and A.J. Williams. *Department of Cardiac Medicine, National Heart and Lung Institute, University of London, London SW3 6LY, UK.*

Calcium plays a primary role in regulating release of calcium from the cardiac sarcoplasmic reticulum (SR) by increasing the open probability (Po) of the calcium-release channel at micromolar concentrations. In the presence of calcium, ATP has been shown to further activate the channel. In the present study, however, we have investigated the mechanisms by which calcium alone, or combinations of calcium and ATP can decrease the open probability of the channel. Vesicles of heavy SR were incorporated into planar phospholipid bilayers and current fluctuations through single calcium-release channels were recorded under voltage clamp conditions. The free $[Ca^{2+}]$ on the *trans-* (luminal) side of the bilayer was 60 mM; *cis-* (cytosolic) free $[Ca^{2+}]$ was varied by adding $CaCl_2$. With calcium as the sole ligand, increasing cytosolic $[Ca^{2+}]$ up to 100 $\mu$M increased channel Po by increasing the frequency of channel opening. Further increases in $[Ca^{2+}]$ resulted in a decline in Po and channels could be completely closed by $[Ca^{2+}]$ in the range 0.5-3 mM. Lifetime analysis indicates that the decrease in Po caused by high $[Ca^{2+}]$ results from a lower frequency of channel opening with no significant alteration to the durations of open events. Channels closed by high calcium (0.5-3 mM) could be re-opened by lowering $[Ca^{2+}]$ to 100 $\mu$M or by addition of the cardiotonic agent sulmazole (1-10 mM).

Similarly, at a constant free activating concentration of calcium (10 $\mu$M), 1 mM ATP increased Po from 0.042 ±0.02 (n=11) to 0.779±0.1 (n=9). However, a further increase in ATP concentration to 5 mM resulted in very rapid flickering events and a decrease in Po to 0.325±0.19 (n=5).

Supported by the British Heart Foundation.

Tu-AM-H3

THE PURIFIED SHEEP CARDIAC SARCOPLASMIC RETICULUM CALCIUM-RELEASE CHANNEL BEHAVES AS A SINGLE ION PORE WITH MONOVALENT CATIONS AS THE PERMEANT SPECIES.

A.R.G. Lindsay, S.D. Manning, A. Tinker and A.J. Williams. *Department of Cardiac Medicine, National Heart and Lung Institute, University of London, London SW3 6LY, UK.*

We have functionally purified the calcium-release channel following solubilisation of sheep cardiac SR membranes with the zwitterionic detergent CHAPS, using a modification of the method described by Lai et al. (*Biochem.Biophys.Res.Comm.*151(1);441-449). Isolated channel proteins were reconstituted into unilamellar liposomes by dialysis. Under voltage clamp conditions the current fluctuations monitored following fusion of the proteoliposomes with planar phospholipid bilayers, were of a single high conductance state. Sub-conductance states were seen in < 5% of the channels incorporated. Single channel slope conductances measured in symmetrical solutions of $Li^+$, $K^+$ and $Na^+$ show saturation with increasing ionic activities. The conductance versus activity plots for the three ion species were found to fit a Michaelis-Menten kinetic scheme. The respective saturating conductances for $Li^+$, $Na^+$ and $K^+$ were calculated to be 248, 516 and 900 pS, with half maximal conductance occurring at 9.1, 17.8 and 19.9 mM. Single channel conductances were also measured for channels exposed to symmetrical mixtures of either $K^+/Li^+$ or $K^+/Na^+$ with a constant total cation concentration of 210 mM. Under these conditions no anomalous behaviour was observed; conductance varied monotonically with mole fraction. Tetramethylammonium and tetraethylammonium act as voltage-dependent blockers from one side of the channel. The effective valence ($z\delta$) for these blockers were measured between 0.44 and 0.55, and 0.85 and 0.90 respectively. Conductance saturation, lack of anomalous mole-fraction behaviour and $z\delta<1$ suggest the sheep SR calcium-release channel behaves as a single ion pore in monovalent cation solutions.

This work was supported by the British Heart Foundation and Medical Research Council.

Tu-AM-H4

$Ca^{2+}$ STORES OF CHICKEN CEREBELLUM PURKINJE CELLS.

P. Volpe[1,2], E. Damiani[2], K. Takei[3], A. Metcalf[3] and P. De Camilli[3]. [1,2]*Department of Physiology and Biophysics, UTMB, Galveston TX,* [2]*Centro di Studio Biologia e Fisiopatologia Muscolare del CNR, Istituto di Patologia Generale, Universita' di Padova, Padova (ITALY), and* [3]*Department of Cell Biology, Yale Universty, New Haven, CT.*

The components predicted to be expressed in intracellular, rapidly-exchanging $Ca^{2+}$ stores of non-muscle cells include a high-affinity $Ca^{2+}$ pump, $Ca^{2+}$ release channels [sensitive to either inositol 1,4,5-trisphosphate ($IP_3$) or $Ca^{2+}$, caffeine and ryanodine] and intraluminal, low-affinity, high-capacity $Ca^{2+}$ binding proteins.

Biochemical analysis indicates the presence of $Ca^{2+}$ pump, calsequestrin (CS) and $IP_3$ receptor in chicken cerebellum microsomes [Volpe et al.(1990) Neuron, in press], and the enrichment of all the putative markers of a $Ca^{2+}$ store in membrane subfractions obtained after isopycnic centrifugation of continuous sucrose gradient.

The existence of structurally specialized subcompartments for $Ca^{2+}$ storage, uptake and release in chicken cerebellum Purkinje cells, is indicated by immunogold labeling of ultrathin cryosections with antibodies specific for CS, $Ca^{2+}$ pump and $IP_3$ receptor.

(Supported by NIH grant GM-40068 and Institutional funds from the Consiglio Nazionale delle Ricerche).

**Tu-AM-H5**

REGULATION OF LYSOSOMAL ION PERMEABILITY BY PROTEIN KINASE C (PKC) IN MACROPHAGES. Gergely L. Lukacs, Ori D. Rotstein and Sergio Grinstein (Intro.by C. M. Deber) Div. of Cell Biology, Hospital for Sick Children and Dept. of Surgery, Toronto General Hospital, Toronto, Canada.

The internal pH of lysosomes ($pH_{ly}$) is determined by the activity of an electrogenic proton pump, a proton leak and counterion conductance. Regulation of the ionic permeability of lysosomal (LY) membranes was studied in thioglycolate-elicited murine peritoneal macrophages. Proton fluxes were estimated fluorimetrically in cell suspensions or in single cells, measuring $pH_{ly}$ in cells loaded with a mixture of fluorescein-dextran and 2,7-dichlorofluorescein dextran by fluid-phase endocytosis. After spontaneous LY acidification attained a steady state ($pH_{ly}$ = 4.6), proton pumping was completely blocked with 500 nM bafilomycin A, a membrane permeant inhibitor of vacuolar $H^+$-ATPases. A slow alkalinization of $pH_{ly}$ was observed upon inhibition of inward $H^+$ pumping, indicating low proton and/or counterion permeability. Addition of conductive protonophores (20 μM CCCP or 1 μM SF6874) markedly accelerated the rate of $pH_{ly}$ increase. In the presence of both bafilomycin A and protonophore, the rate of proton efflux from LY was limited by the counterion conductance. Accordingly, addition of valinomycin or gramicidin accelerated the rate of $pH_{ly}$ change. The rate of alkalinization in bafilomycin A- and protonophore-treated LY, taken as a measure of counterion conductance, was elevated when cells were preincubated with β-12-O-tetradecanoylphorbol 13-acetate (βTPA; 5 nM) or with dioctanoylglycerol (1 μM) by 62.7 ± 2.5 % (mean, S.E., n=8) and 77.9 ±13.2 % (n=3), respectively. Platelet-activating factor (100 nM), a physiological stimulus of macrophages, had a similar effect. In contrast, pretreatment with the inactive αTPA or α-phorbol-12,13-didecanoate was ineffective. One of the counterions participating in the PKC-activated proton efflux is likely to be $Cl^-$, as the the stimulatory effect of PKC could be prevented by the $Cl^-$ channel blocker 5-nitro-2-(3-phenylpropylamino)benzoate (NPPB). The data suggest that, in intact macrophages, LY counterion (likely $Cl^-$) permeability can be modulated by protein kinase C.

**Tu-AM-H6**

PERMEABILITY PROPERTIES OF THE CLOSED STATE OF THE MITOCHONDRIAL OUTER MEMBRANE PORE: INHIBITION OF INTERMEMBRANOUS KINASES AND RECONSTITUTION EXPERIMENTS. R. Benz[1] and D. Brdiczka[2], [1]Lehrstuhl für Biotechnologie, Universität Würzburg, Röntgenring 11, D-8700 Würzburg and [2]Fakultät für Biologie, Universität Konstanz, D-7750 Konstanz, F.R.G.

The outer mitochondrial membrane pore at a voltage above 20-30 mV can adopt a low conductance state which may restrict free permeability of mitochondrial substrates. In order to obtain insight into the physiological meaning of this property we took advantage of the fact that the low conductance pore state could be induced by a polyanion in lipid bilayer membranes and intact mitochondria. Upon reconstitution in artificial bilayers the pore in this substate became exclusively cation selective when the polarity of the applied voltage was negative on the cis side. This behaviour of the pore would explain why induction of the low conductance pore state in intact mitochondria led to a complete inhibition of mitochondrial intermembranous kinases, such as creatine kinase and adenylate kinase, but not of peripheral kinases, for example hexokinase, when utilizing external ATP. The possibility that the inner membrane potential might be transduced to the outer membrane in the contact sites, suggests the existence of cationically selective channels in these sites. This aspect may be important in the regulation of peripheral kinases like creatine kinase, nucleoside diphosphate kinase and adenylate kinase which are located behind the mitochondrial outer membrane.

**Tu-AM-H7**

IMMUNOLOGICAL IDENTIFICATION OF THE 32kDa AND 30 kDa PROTEINS WHICH CO-PURIFY WITH THE PERIPHERAL BENZODIAZEPINE (pBz) RECEPTOR OF RAT KIDNEY MITOCHONDRIA. M.W. McEnery, A.M. Snowman, E.E. Thompson, and S.H. Snyder, Dept. of Neuroscience, The Johns Hopkins Univer. School of Medicine, Baltimore, MD 21205

The mitochondria of numerous peripheral tissues (kidney, adrenal, ovary) have been shown to possess a membrane-bound receptor which binds benzodiazepines (diazepam, Ro5-4864) and isoquinoline carboxamides (PK11195, PK14105) with nanomolar affinities. We have purified this peripheral benzodiazepine (pBz) receptor complex from rat kidney mitochondria and demonstrate the receptor to be comprised of three non-identical subunits with apparent molecular weights of 32, 30 and 18 kDa. The intact purified complex exhibits pharmacological properties indistinguishable from the membrane-bound receptor. Antisera were raised against the pBz complex in rabbits, resulting in the production of two different antisera specific for either the 32 kDa or the 18 kDa component. The anti-32 kDa antisera has been shown by two-dimensional electrophoresis to be specific for a family of 32 kDa proteins which can be labelled by 14C-DCCD. It is very likely, therefore, that the 32 kDa antigen present in the purified pBz receptor is the voltage activated anion channel (VDAC) and our anti-32 kDa antiserum is anti-rat kidney VDAC. The 30 kDa component of the pBz receptor was recognized by a second antibody against the ADN carrier. Western blot analysis confirmed the 32 kDa and 30 kDa protein to be present only in the fractions of the purification which possess high specific activity ligand binding. The identify of the 32 kDa and 30 kDa subunits of the intact pBz receptor were verified further through the use of anti-phosphate carrier antiserum which exhibited a markedly different pattern of immunological labelling than either anti-VDAC or anti-ADN carrier antisera. These results indentify the ADN carrier and VDAC as the proteins which co-purifiy with the pBz receptor and imply an auxilliary function for both the ADN carrier and VDAC.

**Tu-AM-I1**

**DIHYDROPYRIDINE RECEPTORS ARE PRIMARILY FUNCTIONAL L-TYPE Ca CHANNELS IN RABBIT CARDIAC MYOCYTES.** W.Y.W. Lew*, L.V. Hryshko & D.M. Bers, Division of Biomedical Sciences, Univ. of Calif., Riverside, 92521 and *Univ. of Calif., San Diego, 92161

In skeletal muscle the density of dihydropyridine receptors (DHPR) was reported to be 35-50 times that of functional L-type Ca channels (Schwartz *et al.*, Nature 314:747-751, 1985). This is consistent with the DHPR functioning as the voltage sensors which induce SR Ca release rather than as Ca channels *per se*. To determine if such a disparity exists in cardiac muscle, we measured DHPR density by [$^3$H]-PN200-110 binding in rabbit ventricular homogenates and isolated myocytes. The DHPR density in homogenate was 75.3 ± 8.3 fmol/mg (SD, $K_d$ = 2.6 ± 0.8 nM, n=6) and in myocytes was 151 ± 5 fmol/mg ($K_d$ = 1.49 ± 0.15 nM, n=4). Assuming 120 mg protein/cm$^3$ heart, 25% extracellular space and a surface/volume ratio of 0.6 $\mu m^{-1}$, the DHPR density estimated from ventricular homogenate is 12.8 DHP sites/$\mu m^2$. Assuming 75% of homogenate protein is from myocytes, 14.6 DHPR/$\mu m^2$ is estimated from myocyte data. The number of functional L-type Ca channels (N) was measured in isolated myocytes using voltage clamp and the formula N = I/(i·$p_o$), where I = peak whole cell current, i = single channel current, and $p_o$ = global open probability. We measured Na current through Ca channels ($I_{ns}$) to prevent $Ca_i$-induced inactivation. Whole cell ($I_{ns}$) was compared with single channel measurements ($i_{ns}$ and $p_o$) under the same conditions (140 mM NaCl, 4 mM EGTA, pH 7.4 at 22°C). Isoproterenol was used to maximize currents and increase $p_o$. From a holding potential of -50 mV, peak $I_{ns}$ was 12.6 ± 6.5 nA or 117 ± 58 pA/pF (n = 7) and occurred at -34 ± 16 mV. Single channel conductance was 40.8 ± 9.1 pS (n = 12) with a calculated $i_{ns}$ of 2.56 pA at -34 mV. The overall $p_o$ was 0.030 ± 0.006 in patches with only a single channel (n = 16). The calculated density of functional L-type Ca channels was 15.1 channels/$\mu m^2$, similar to the DHPR density. We conclude that in cardiac muscle the density of DHPR is similar to that of L-type Ca channels, consistent with the requirement for Ca influx in cardiac E-C coupling.

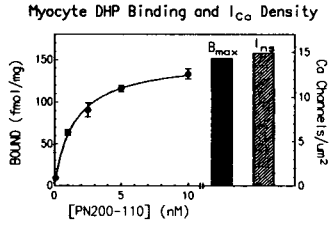


**Tu-AM-I2**

**DIFFERENT EFFECTS OF PERCHLORATE ON SKELETAL MUSCLE EC COUPLING, CARDIAC Ca GATING CURRENTS AND GATING OF DHP RECEPTORS IN BILAYERS.** E. Ríos, R. Shirokov, R. Levis, A. González, I. Stavrovsky, J. Ma, *C. Mundiña-Weilenmann and *M.M. Hosey. Rush University and *Northwestern University, Chicago, IL.

$ClO_4^-$ is an effective agonist of EC coupling in skeletal muscle, believed to act primarily on the voltage sensor. At 8 mM it shifts the activation curves of charge movement and Ca release to the left by ≃ 25 mV (Lüttgau et al. 1983; González et al., this meeting). We determined effects of $ClO_4^-$ on two other manifestations of dihydropyridine receptors (DHPrs): voltage-sensitive currents through channels from skeletal T membrane vesicles fused in bilayers and Ca gating currents in heart myocytes. The voltage-dependent activation of DHPr channels in bilayers ($P_o$ *vs.* V, Mundiña-Weilenmann et al., this meeting) was described by a Boltzmann with parameters: $P_{max}$=9.2%, K=5.9 mV and $V_T$=-23 mV. $ClO_4^-$ shifted slightly the distribution to a *higher* voltage ($P_{max}$=13.9, K=5.9 mV, $V_T$=-16 mV). The differences were significant. Cardiac gating currents were measured in enzymatically dissociated ventricular myocytes from the guinea pig (Shirokov et al., this meeting). A major fraction of the mobile charge could be assigned to gating currents of Ca channels and followed a Boltzmann function of voltage ($Q_{max}$=12nC/$\mu$F, K=10mV, $V_T$= -20mV). $ClO_4^-$ reduced $Q_{max}$ to 10nC/$\mu$F and shifted the voltage dependence by -7mV, without changing the steepness. Thus $ClO_4^-$ has a clear agonist effect only in skeletal muscle.

The DHPrs in skeletal fibers are coupled physiologically to Ca release channels; those in the bilayer experiments or in the cardiac cell are not. That $ClO_4^-$ does not have its agonist effect in these two preparations suggests that the DHPrs acquire different properties when they are in physiological interaction with the release channels.

Two possibilities are considered: that $ClO_4^-$ is a primary agonist of the release channel, and potentiates charge movement secondarily through the positive feedback process that generates $I_\gamma$ (Pizarro et al., this meeting) or that the voltage sensor acqires new reactivity through mechanical interaction, direct or indirect, with the release channel. Supported by NIH, MDA and AHA.

**Tu-AM-I3**

**SKELETAL MUSCLE DIHYDROPYRIDINE AND RYANODINE RECEPTOR PROTEINS INTERACT IN BILAYERS.** J. Ma, M.M. Hosey* and E. Ríos (intro. by B. Eisenberg). Rush University and *Northwestern University, Chicago, IL.

Rabbit skeletal muscle T membrane vesicles, fused with planar bilayers, give rise to DHP-sensitive single channel currents. When the membrane is kept steadily polarized at -80 mV (H.P.), the channels remain closed, and open upon pulse depolarization beyond -40 mV (Mundiña-Weilenmann et al., this meeting). Ensemble averages of these currents reveal voltage- and time- dependent activation, inactivation and deactivation. The kinetics follow $I \propto m^3h$, where m and h are H-H variables with $\tau_m$ = 118 ms (st. err.fit = 4 ms,) and $\tau_h$ = 1.24 s (0.04 s) at -10 mV and 22°C. Upon repolarization the channels close with time constant ≃ 8 ms. The $P_o$ (open probability) *vs.* V is a Boltzmann of parameters $P_{max}$=7.6% (st.dev.=2.4, n=7), K=6.7mV (1.1), $V_T$=-26mV (2.3).

Upon *cis* (intracellular) addition of purified ryanodine receptor (kindly supplied by Dr. G. Meissner) the kinetics and voltage distribution changed. Gating became faster: $\tau_m$ was reduced to ≃ 50 ms, $\tau_h$ did not change and deactivation became too fast to be resolved. The figure shows ensemble averages and fits for a 400 ms pulse. $P_{max}$ increased to 17.8% and the other Boltzmann parameters did not change (n=5). Ryanodine receptor that was boiled, heated to 70°C, or added to the *trans* side had no effect.

These effects report an interaction between the added RYrs and DHPrs in bilayers, which may or may not reflect physiological events. Supported by NIH, MDA and AHA.

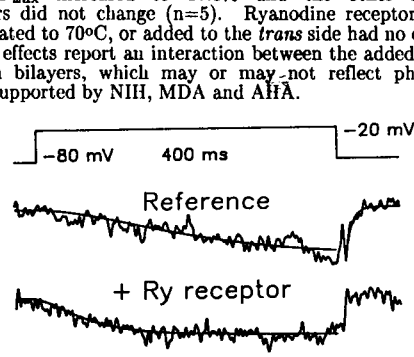


**Tu-AM-I4**

**SODIUM CURRENTS IN SKELETAL MUSCLE FIBERS OF *MDX* AND CONTROL MICE.**

*C. Mathes, R. E. Weiss, and F. Bezanilla.*
Dept. of Physiology, UCLA, Los Angeles, CA 90024

The activation and inactivation properties of macroscopic Na currents in cell-attached patches on the surface of depolarized EDL (*extensor digitorum longus*) muscle fibers were compared in *mdx* (dystrophic mouse model), C57BL/10SnJ (*mdx* control strain) and white mice. The half-inactivation voltages ($V_{1/2}$), determined by fitting a single Boltzmann distribution to the fraction of peak current versus pre-pulse voltage, were similar in all three groups. The values were: $V_{1/2}$= -91.3 ±3.1 mV (mean ± s.d., n=10 patches, *mdx*), -93.0 ±5.1 mV (n=12, *mdx* controls), and -99.6 ±4.4 mV (n=12, white mice). The half-maximal activation voltages of the normalized peak conductances (obtained by interpolation) were -48 ±3.5 mV (n=7, *mdx*) and -45 ±3.7 mV (n=5, *mdx* controls). The effective gating charge (z), estimated by the limiting slope of a semi-log plot of the activation curve, was 4.7 ± 0.4 (*mdx*) and 3.7 ±0.3 (*mdx* controls). The voltage range over which activation and inactivation of the Na currents occurred in our experiments was more negative than the majority of previously reported values. Peak Na currents ranged from 20 to 330 pA per patch. The maximum current measured from patches excised into the bath medium decreased to 47.0% (± 21%, n=14) of the pre-excision values within 5 to 10 minutes. Gigaseals were obtained on the surface membrane of single fibers dissected from EDL muscles following mild collagenase treatment (1 hour). Muscles were obtained from adult mice (4-6 weeks). Single fibers were transferred to an experimental chamber containing (in mM): 142 KCl (or CsCl), 10 NaCl, 0.2 $CaCl_2$, 0.5 EGTA, 2 $MgCl_2$, 10 HEPES, and 5 glucose (pH 7.3). The pipette solution contained: 142 NaCl, 2 $CaCl_2$, 2 KCl,1 $MgCl_2$, 10 HEPES, and 5 glucose (pH 7.3).

[Supported by the Muscular Dystrophy Association and the American Heart Assn.]

**Tu-AM-I5**

DIHYDROPYRIDINE BLOCK OF CHARGE MOVEMENT IN NORMAL BUT NOT DYSGENIC MYOTUBES. B.A. Adams and K.G. Beam, Dept. of Physiology, Colorado State University, Ft. Collins, CO, 80523.

The muscular dysgenesis mutation in mice appears to alter the gene for the skeletal muscle dihydropyridine (DHP) receptor. Recently, we reported that immobilization-resistant charge movement in dysgenic skeletal muscle myotubes ($Q_{dys}$) is only about one-third as large as that present in normal myotubes ($Q_{norm}$) and has a different voltage-dependence (Adams et al., 1990; Nature 346:569). To further characterize $Q_{dys}$ and $Q_{norm}$, we have examined their relative sensitivities to the DHP antagonist (+)-PN 200-110. Dysgenic and normal myotubes were voltage-clamped using the whole-cell technique. Steady holding potential was -80 mV. The voltage protocol consisted of a 1 s prepulse to -30 mV and a subsequent 20 ms repolarization to a pedestal potential of -50 mV (to immobilize sodium channel and fast calcium channel gating charge and to prevent their recovery, respectively). The control pulse was a step from -80 to -120 mV. Temperature was 20-22 °C. Under these conditions, application of 10 uM (+)-PN 200-110 reduced $Q_{dys}$ by only 7 ± 3% (mean ± sem; n=8). In contrast, this same concentration of (+)-PN 200-110 reduced $Q_{norm}$ by 41 ± 3% (n=11). These results pharmacologically distinguish $Q_{dys}$ from $Q_{norm}$. Interestingly, evoked twitches of normal myotubes bathed in physiological saline appeared unaffected by application of either 10 uM (+)-PN 200-110 or nifedipine. Thus, in future experiments it will be important to determine the effects of DHPs on $Q_{norm}$ and contraction under identical conditions.

Supported by NIH Fellowship NS 08567 to B.A. and NS 24444 to K.B.

**Tu-AM-I6**

Muscle fibers of dysgenic muscle in vivo lack a surface component of peripheral couplings. Clara Franzini-Armstrong, Martine Pincon-Raymond* and Francois Rieger* Univ. Pennsylvania, Philadelphia Pa. and *Unite 153, INSERM, Paris, France.

Muscle dysgenesis is a lethal recessive mutation in mice. Muscle fibers in the homozygous mutant have normal action potentials and can develop local contractions and tension, but lack excitation-contraction coupling. The defect is associated with a major decrease in slow calcium current and in expression of the $_1$ subunit of the dihydropyridine receptor (DHPR). We have studied the in vivo development of diaphragm in mdg/mdg embryos, with the aim of defining how well transverse (T) tubules and junctions between sarcoplasmic reticulum (SR) and T tubules/surface membrane develope. T tubules were "stained" and examined in semithin sections; the structure of peripheral couplings was studied by freeze-fracture. In mdg/mdg embryos at perinatal ages T tubules are less frequent and have a less mature disposition than in control muscles; rare triads have orderly disposed rows of feet; calsequestrin is associated with the feet-bearing junctional SR membrane. In normal muscles at early stages of development sites of peripheral couplings are marked by the presence of large particles, forming small groups of four (tetrads). Junctional tetrads of peripheral couplings and triads are associated with the underlying junctional feet to form a complex which spans the entire SR-to-surface junction. In mdg/mdg mutants tetrads are absent, indicating that DHPR may be their constituent protein. Interestingly, tetrads of peripheral couplings are in a 1:1 ratio to junctional feet, differently from the 1:2 ratio so far found in triads of adult muscle. Supported by MDA and INSERM.

**Tu-AM-I7**

GROWTH FACTORS REGULATE THE RYANODINE RECEPTOR/JUNCTIONAL CHANNEL COMPLEX, DHP RECEPTOR, CONTRACTILE PROTEINS AND CELL MORPHOLOGY IN A MYOGENIC CELL LINE

Andrew R. Marks, Akitsugo Saito, Yan Dai, Sidney Fleischer and Mark B. Taubman. Brookdale Center for Molecular Biology, Mount Sinai Medical Center, NY, NY 10029 and Dept. of Molecular Biology, Vanderbilt University, Nashville, TN 37235

We examined the regulation of the ryanodine receptor/junctional channel complex (JCC, foot structure) of the sarcoplasmic reticulum (SR) and associated muscle specific genes in the murine myogenic cell line BC3H1. The JCC mRNA accumulation (by Northern blot) and protein (by electron microscopy) were negatively regulated by fibroblast growth factor (FGF) within 48 and 120 hours respectively. The dihydropyridine-sensitive calcium channel (DHP-CC), α-tropomyosin, and skeletal α-actin mRNAs (by Northern blot) and myofibril formation (by electron microscopy) were also negatively regulated by growth factors (GF) with a time course similar to that seen for the JCC. Moreover,withdrawal of GF stimulates a dramatic shape change (cells elongate) in BC3H1 which may be equivalent to contraction. FGF inhibits expression of the myogenic factor myogenin in BC3H1 cells but the mechanism of inhibition of muscle cell differentiation remains unclear. These data suggest that there is a common (multifactorial) regulatory pathway governing the expression of the calcium handling gene products, JCC, and DHP-CC, as well as the contractile protein genes and that the expression of these genes is associated with profound changes in cell morphology.

**Tu-AM-I8**

TOXINS OF EXCITATION-CONTRACTION COUPLING: P. IMPERATOR SCORPION VENOM INHIBITS [$^3$H]RYANODINE BINDING AND CLOSES Ca RELEASE CHANNELS OF SARCOPLASMIC RETICULUM. Hector H. Valdivia. Department of Physiology, University of Wisconsin, Madison, WI, 53706.

The [$^3$H]Ryanodine binding assay made possible the purification of ryanodine receptors from the SR of striated muscle and the identification of this 565 kDa protein as the Ca release channel. However, the extremely slow association and dissociation kinetics, the ambiguous effects depending on concentration, and the $Ca^{2+}$-dependence of binding, restrict the use of ryanodine as a tool to dissect the contribution of ryanodine receptors to excitation-contraction coupling. In a search for novel ligands of ryanodine receptors, we found that the venom of the african scorpion *P. imperator* specifically inhibited [$^3$H]Ryanodine binding to cardiac and skeletal muscle SR and to brain microsomes. A chromatographic fractionation of the venom showed that more than 90% of the inhibitory activity was concentrated in a fraction containing several polypeptides of $M_r$ ~10 to 14 kDa. This partially purified fraction inhibited [$^3$H]Ryanodine binding with an $IC_{50}$ of 0.2 μg/ml. Assuming an active component of molecular weight ~10 kDa and 25% purity, we estimated a dissociation constant of the polypeptide-receptor complex of ~5 nM. A similar $IC_{50}$ was obtained in a solubilized preparation of SR, suggesting that inhibition occurred through a direct interaction with the ryanodine receptor or with a tightly associated protein that regulates its conformational state. In recordings of ryanodine receptors in planar bilayers, the semi-purified fraction reduced the burst time and the mean open time without effecting the unitary channel conductance. *P. imperator* venom opens new avenues in the pharmacological dissection of the functional role of Ca release channels. Supported by NIH, AHA, MDA, CFF.

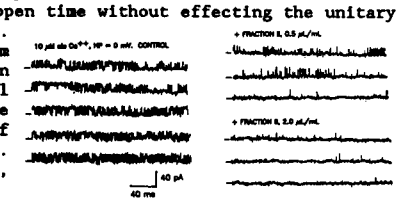

Tu-AM-J1

## A NATURAL DECONVOLUTION OF CIRCULAR DICHROISM SPECTRA OF PROTEINS.

G. Fasman, A. Perczel, G. Tusnády and M. Hollósi. Graduate Dept. Biochemistry, Brandeis University, Waltham, MA, USA; Dept. of Organic Chemistry, Eötvös University, Budapest; and Mathematical Institute of Hungarian Academy of Sciences, Budapest, Hungary.

A new algorithm, called convex analysis, has been developed to deduce the chiral contribution of the common secondary structures directly from experimental circular dichroism (CD) curves of a large number of proteins. The analysis is based on CD data reported by Yang, J.T., Wu, C.-S.C., and Martinez, H.M. [*Methods in Enzymol.* 130, 208-269 (1986)]. Application of the decomposition algorithm for simulated protein data sets resulted in component spectra [$B(\lambda, i)$] identical to the originals and weights [$C(i, k)$] with excellent Pearson correlation coefficients ($R$) [Chang, C.T., Wu, C.S.C. & Yang, J.T. (1978) *Anal. Biochem.* 91, 12-31]. Test runs were performed on sets of simulated protein spectra created by the Monte Carlo technique using poly-L-lysine based pure component spectra. The significant correlational coefficients ($R > 0.9$) demonstrated the high power of the algorithm.

The algorithm, applied to globular protein data, independent of X-ray data, revealed that the CD spectrum of a given protein is composed of at least four independent sources of chirality. Three of the computed component curves show remarkable resemblance to the CD spectra of known protein secondary structures. This approach yields a significant improvement in secondary structural evaluations when compared to previous methods, as compared to X-ray data, and yields a realistic set of pure component spectra. The new method is a useful tool not only in analyzing CD spectra of globular proteins, but also has the potential for the analysis of integral membrane proteins.

Supported by NSF.

Tu-AM-J2

## MULTIPLE CONFORMATIONS OF THE fd PHAGE COAT PROTEIN

A. Keith Dunker, Gregory Arnold, and Linda Roberts, Department of Biochemistry and Biophysics, Washington State University, Pullman, WA 99164-4660

The fd phage coat protein (8P) contains 50 amino acids and is predominantly helical. The bulk of the fd capsid consists of a tight, interlocking network of about 2,700 copies of the 8P protein in closely packed layers with their axes inclined about 20° relative to the particle axis.

The CD spectrum of the native phage has a highly unusual shape, with 208 nm and 222 nm bands typical of a helix, but with the 222 trough being significantly deeper than the one at 208 nm. Previous interpretations ascribed the unusual spectral shape to optical distortions (absorptive flattening and/or differential light scattering) arising from the large particulate size of the phage as compared to a protein uniformly disbursed in solution. However, we presented data showing that the anomolous CD intensities arise, not from optical artifacts, but rather from tryptophan absorption. Namely, CD, Raman, UV and fluorescence studies on the oxidation of the fd phage by N-bromosuccinimide (NBS) indicate that, at low concentrations, NBS specifically oxidizes the 8P tryptophan without altering the secondary structure of 8P and, concomitantly, eliminates the anomolous spectral shape.

Treatment of fd with chloroform at low temperatures leads to contraction of the phage to a rod, called I-form, which is about 1/3 the length of the original phage. Exposure of the I-form to chloroform at higher temperatures leads to further contraction to a spherical shaped structure, called spheroids by others and S-forms by us. These morphological changes might mimic the steps involved insertion of the 8P protein into the membrane during phage infection.

Here we report that the CD spectrum of I-form is remarkably like that of NBS-treated phage, which suggests that contraction from phage to I-form probably involves rearrangement of the helical subunits with little or no change in their backbone structures. The CD spectrum of S-form is almost identical to that of 8P in artificial membrane bilayers, suggesting that the protein in S-form might be much like that in bilayers, but without the surrounding lipid.

Tu-AM-J3

## CONFORMATIONAL CHANGE OF α-BUNGAROTOXIN UPON BINDING TO PEPTIDES MIMICKING THE MAIN CHOLINERGIC BINDING SITE OF THE NICOTINIC ACETYLCHOLINE RECEPTOR.

Antonio Bertazzon and Bianca M. Conti-Tronconi
Department of Biochemistry, College of Biological Sciences, University of Minnesota, St. Paul, MN 55108.

The secondary structure of peptides mimicking the main cholinergic binding site of the nicotinic acetylcholine receptor (nAChR) has been investigated by circular dichroism (CD) and fluorescence spectroscopy. A synthetic peptide corresponding to the sequence segment 181-200 of the a subunit of Torpedo nAChR, and a panel of peptide analogues carrying single residue substitutions of this sequence segments, were used.

Substitution of large residues, such as $Arg_{183}$ or $Trp_{184}$, increased the flexibility of the corresponding peptides, which had a higher content in the signal of β or α components in the CD spectrum. The two adjacent cysteines at positions 192 and 193, as well as $Pro_{197}$ and $Tyr_{198}$, were found to be important in the maintenance of the secondary structure of the peptides in solution.

Binding of α-bungarotoxin (α-BTX) to the peptides caused an increase of the total content of β-structure of the complex, suggesting that a conformational change occurs upon binding. Investigation of formation of the complex in the presence of an excess α-BTX, or of an excess of binding peptide, suggests that the observed conformational change occurs mostly, if not completely, within the α-BTX molecule.

The behavior of the maximum emission wavelength of the intrinsic fluorescence of the two tryptophanyl residues of the peptide in solution suggests that these residues are surrounded by a hydrophilic environment, which does not change after binding to α-BTX.

A computer generated model, based on these experimental observations, is discussed.

Tu-AM-J4

## HELIX-COIL TRANSITIONS IN VARIOUS HUMAN β-TROPOMYOSINS: INFLUENCE OF THE MEDIUM.

C. Ferraz*, J. Sri Widada*, J.P. Liautard* and F. Heitz**
* CRBM-CNRS and INSERM-U.249 F. 34033 Montpellier Cedex
** LPCSP-CNRS B.P. 5051 - F.34033 Montpellier Cedex France

The nature of the forces involved in the stabilization of protein structures is still matter of debate and their determination requires investigations on model systems such as synthetic peptides or natural proteins of well defined conformation. In this field β-tropomyosin appears as a good model for such a study as it adopts a fully α-helical coiled coil conformation stabilized through interchain hydrophobic interactions. The development of genetic engineering allowing the obtention of mutants provides a further tool for the elucidation of the role of various residues or of some sequences on the conformational stability of the tropomyosin molecule.

We show here that the deletion of either the 21 N- or 31 C-terminal residues does not modify the thermal stability of tropomyosin. However, these deletions reduce the stability toward chaotropic agents such as guanidinium chloride (≈ 1M for the C-terminus modified mutant which has to be compared with 3M for the wild type). The thermal stability is lowered by the presence of acetonitrile (≈ 10° C for 28%) while it is increased by methanol (≈10° C for 28%). The possibility of formation of heterodimers has also been examined under the same conditions. While it follows the thermal denaturation observed by CD in 0.1 M NaF and in presence of acetonitrile, it preceeds the helix-coil transition when methanol is present in the medium. This observation indicate that formation of a coiled coil structure is not determinant for the thermal stability of an α-helix and suggest that the structure of the surrounding water could play a major role in the stability of this type of structure.

Tu-AM-J5

**PHYSICOCHEMICAL, HOMOLOGY, CD, AND SECONDARY STRUCTURE ANALYSIS OF HUMAN APOLIPOPROTEINS A-I, A-IV, AND E-3.** Robert T. Nolte & David Atkinson, Dept of Biophysics, Boston University School of Medicine, Boston, MA

The serum apolipoproteins are a diverse family of proteins responsible for lipoprotein particle structure, cellular targeting, and activation of enzymes involved in lipid metabolism. We have used an integrated approach to structure prediction to examine the sequence of the major plasma apolipoproteins A-I, A-IV, and E-3. Methods and programs have been developed to 1) identify statistically significant sequence homologies on the basis of conservative substitutions and similarities in physicochemical properties; and 2) calculate the local mean, hydrophobic moment, and 1D Fourier spectra from the physicochemical properties. Secondary structure prediction was carried out using the established methods of Chou, Fasman, & Prevelige (Prediction of Protein Structure and the Principles of Protein Conformation. Ed. Fasman. 1989), Garnier, Osguthorpe, & Robson (J. Mol. Biol. 120:97-120. 1978), Gascuel & Golmard (CABIOS 4:357-365. 1988) and Whitlow & Teeter (Proteins 4:262-273. 1988). Circular dichroic data on purified lipid-protein complexes was analyzed by the method of Mao & Wallace (Biochemistry 23:2667-2673. 1984) to provide a secondary structure constraint for the final prediction. We have developed a refined consensus sequence for the two previously described tandem 11-AA repeats found in these sequences. Our A/B repeat assignments differ from those reported previously and change the assignment of 3 segments in A-I, 5 in E-3, and 3 in A-IV. The Pro at position 1 was found to be the major determinant of the A-type repeat with an Ala in the corresponding position in B-type repeat. Position 2 was found to be the least determined position for either repeat. The integration of these results into a single secondary structure model for each protein in general supports the concept of the amphipathic helix as an important motif of lipid interaction for these proteins. However the analysis also suggests that not all tandem 11-AA repeats fold into the amphipathic helical structure punctuated by proline turns as previous models have proposed. Several repeats may adopt alternative secondary structures. Several relatively non-amphipathic apolar helices have been found which may also play a role in the binding of these proteins to the plasma lipoprotein particles.

Tu-AM-J6

**DYNAMIC SHAPES OF IMMUNOGLOBULINS REVEALED BY FLUORESCENCE RESONANCE ENERGY TRANSFER** Y. Zheng, *B. Shopes, D. Holowka and B. Baird. Cornell University, Ithaca, NY and *Stanford University, Stanford, CA

Average energy transfer distances between eosin-dansyl and fluorescein-dansyl in the two anti-dansyl combining sites at the tips of the Fab arms were found to be ≥95 Å for murine IgE and ≥85 Å for human IgG1. These correspond to an average angle of ≥60° between the Fab moieties for both intact antibodies. The distance distributions between the anti-dansyl combining sites and the C-terminal end of Fc segment of IgE and IgG1 were determined by varying the Forster critical transfer distance ($R_0$) by collisional quenching of donor probes with $I^-$. The antibodies were labeled with fluorescein maleimide at genetically engineered cysteine residues near their C-terminal ends, and energy transfer between these sites and eosin-dansyl in the combining sites had unexpectedly large efficiencies of 0.20 for IgE in solution, 0.22 for IgE bound to its high affinity Fc receptor, and 0.15 for IgG1 in solution. Analysis of the $R_0$-dependent transfer efficiencies revealed that the half-width of the IgE distance distribution changes from 26 Å to 14 Å when IgE binds to its Fc receptor on cell membranes, while the average distance remains virtually unchanged at 75 Å. The half-width of the distance distribution for IgG1 in solution is 75 Å with an average separation distance of 95 Å.

These results indicate that IgE is bent in a relatively compact conformation that becomes even more rigid upon binding to its receptor. In contrast, IgG1 appears to have more internal segmental motion that accounts for the rather short average distance between the tips of the Fab and Fc segments. Supported by NIH Grants AI18306 and AI22449, by Cornell Biotechnology Fellowship (Y.Z.), and by Leukemia Sciety of America Fellowship (B.S.).

Tu-AM-J7

FLUORESCENCE INVESTIGATIONS ON MITOCHONDRIAL MALATE DEHYDROGENASE SUBUNIT INTERACTIONS. Robert H. McKay and David M. Jameson, Department of Biochemistry and Biophysics, University of Hawaii, Honolulu, HI 96822.

The dimer-monomer equilibrium of pig heart mitochondrial malate dehydrogenase (mMDH), a 70,000 dalton protein, has been investigated using fluorescence methodologies. Highly active fluorescein labeled mMDH was obtained using affinity chromatography with an Affigel Red resin. The fluorescence parameters including lifetime and both steady-state and dynamic polarizations were characterized. The dynamic polarization data indicated a Debye rotational relaxation time in the range of 110-120 nanoseconds which is consistent with a slightly ellipsoidal dimeric protein. The steady-state polarization was found to decrease with increasing fluorescein labeling suggesting energy transfer between the fluorophores. The concentration dependence of the steady-state polarization demonstrates that, in the pH range of 8.0 to 5.5, at 20°C and at ionic strengths near 0.1 M, the dissociation constant for the dimer-monomer equilibrium is subnanomolar. This system is also being investigated using gel-filtration chromatography. At high concentrations (~$10^{-5}$ M) the protein dissociates in the presence of 1.0 M guanidinum chloride; upon dilution of this denaturant the dimer forms again very rapidly (as judged by the steady-state polarization) while the enzyme activity takes appreciably longer to return. These observations are considered in light of the controversy in the literature concerning the dissociation characteristics of mMDH and in terms of the conformational drift hypothesis. Supported by National Science Foundation grant DMB-9005195.

Tu-AM-J8

**DYNAMICS OF MELITTIN IN DIFFERENT CONFORMATIONAL STATES DETECTED BY FREQUENCY DOMAIN FLUOROMETRY.**
Ettore BISMUTO, Ivana SIRANGELO and Gaetano IRACE, Dipartimento di Biochimica e Biofisica, Università di Napoli, Italy.

Melittin is a cationic amphiphilic peptide with a random coiled structure in water free of inorganic salts. At high ionic strength and neutral pH, it aggregates forming a tetrameric complex. Due to its positive changes, melittin molecule strongly binds to negative charged membrane, as a single chain, adopting an *a* -helical conformation. Because of its ability to exist in different aggregate and conformational states, melittin is an excellent candidate to investigate the relation between dynamical and structural aspects of polypeptide conformations. Furthermore, melittin has a single tryptophan without any tyrosine residue so that fluorescence techniques (specifically, multifrequency phase shift and demodulation fluorometry) provide a very useful window for observing the dynamics of processes occurring on nanosecond time scale. In this communication, we examine the temperature dependence of the fluorescence emission of decay of melittin in the monomeric and tetrameric structure as well as in reversed sodium bis(2-ethyl-1-exyl)sulfosuccinate micelles in n-heptane with a different water content. These water in oil microemulsions represent a simple model to study the biological events occurring at the membrane interface.
The results are discussed in terms of a different conformational freedom of polypeptide as a consequence of changes in the structural organization, solvent composition or temperature.

**Tu-AM-K1**

MEMBRANE PERTURBING AGENTS, INCLUDING FLUIDIZERS, SIGNIFICANTLY AFFECT ELECTROFUSION YIELDS IN ERYTHROCYTE GHOST MEMBRANES. M.-P. Rols* and Arthur E. Sowers, Cell Biology, ARC/Holland Laboratory, Rockville, MD 20855.

Many previous studies of biomembrane fusion have utilized fusogenic chemicals to induce fusion. Our efforts to understand the electrofusion mechanism, and any relationship it may have with biological or other fusions have led us to survey the hypothesis that the fusion yield in rabbit erythrocyte ghosts caused by a fusogenic electric field pulse may be altered in different ways by chemical agents which are or are not fusogenic themselves. Alcohols (C-1 to C-4) all increase fusion yield up to 20% for solution strengths up to 20% v/v. The exception is butanol which causes a reproducible strong fusion yield peak at 0.01 % v/v, followed by a decrease in fusion yield at higher concentrations. All alcohols caused noticeable increases in lateral diffusion rates. Lysophosphatidyl choline caused a uniform decrease in fusion yield at all monotonically increasing concentrations. However, the lyso-PC-induced inhibition of fusion yield was strongly dependent on the decay half-time of the fusogenic electric field pulse and, also, at very low lyso-PC concentrations (1.5 ug/ml) in the buffer. The presence of magnesium or calcium in the hemolysis buffer, reported to preserve or reduce transmembrane asymmetry in erythrocyte ghosts (Connor et al., BBA 1025:82 [1990]), had little (not significant) or inhibiting, respectively, effects on fusion yield suggesting that membrane asymmetry favors fusion, although other effects from calcium cannot be ruled out. The presence of buffer viscosity-increasing chemicals (ethylene glycol, sucrose, or glycerol) all strongly inhibited fusion yield. *Permanent address: CRBGC/CNRS, 31062 Toulouse, France. Supported by ONR grant N00014-89-J-1 to AES.

**Tu-AM-K2**

MEMBRANE FUSION VS. TRANSFER IN VIRAL FUSION MONITORED BY THE FLUORESCENT PROBE OCTADECYL RHODAMINE (R18)

Christopher Di Simone and John D. Baldeschwieler, Noyes Lab., 127-72, Division on Chemistry and Chemical Engineering, California Institute of Technology, Pasadena, CA 91125

The probe octadecyl rhodamine has been used by a number of workers to examine membrane interactions. We have been using the probe to examine fusion of native and reconstituted mumps and Sendai virus with mammalian cells. We have been interested in distinguishing between fusion and transfer behavior. The effects of various 'fusion inhibitors' on viral fusion will be discussed. We have compared the viral fusion rates given by R18 with other fluorescent membrane probes. We have also attempted to compare contents mixing with membrane mixing rates.

In addition a simple formula for correcting fusion values for non-infinite dilution into target membranes will be presented.

A common assumption in experiments with R18 is that addition of Triton X-100 detergent at the end of the experiment will give infinite dilution values. This assumption has been tested and the results will be presented.

This work has been supported by the Caltech Consortium in Chemistry and Chemical Engineering ; Founding Members: E. I. du Pont de Nemours and Company, Inc., Eastman Kodak Company, Minnesota Mining and Manufacturing Company, Shell Oil Company Foundation.

**Tu-AM-K3**

**SIALIC ACID IS REQUIRED FOR THE pH DEPENDENCE OF INFLUENZA A/PR/8/34 VIRUS FUSION WITH PLANAR LIPID MEMBRANES.** W.D. Niles and F.S. Cohen. Department of Physiology, Rush Medical College, Chicago, IL.

We are using video fluorescence microscopy to study binding and fusion of influenza virus to planar membranes mediated by the viral hemagglutinin glycoprotein (HA). It is well-known that cell infection by influenza, which occurs by fusion of the viral envelope membrane with a cell membrane, is strongly promoted at low pH. We have found that pH-dependent fusion of influenza virus with planar membranes requires sialic acid on the planar membrane surface. The fusion rate to phospholipid membranes, made of either asolectin or purified phospholipids but containing no gangliosides, is about 6 fusion events/min and this rate is independent of pH. With globosides, which have tetra-galactose headgroups but do not possess sialic acid, the fusion rate is similarly pH independent. However, we observe pH-dependent fusion with the gangliosides GD1a + GT1b, GM1a, or GM3, all of which possess sialic acid. The fusion rate at pH 7.4 is about 2/min, and, as the pH is lowered to within the range of 5.6 to 5.4, this rate is augmented to about 40/min. At pH < 5.4, the rate continues to increase. Sialic acid, known to be the receptor determinant for virion binding to target membranes, binds to HA at a well-characterized site in the HA1 subunit, which is distal to the viral envelope. The domain which triggers fusion, however, is located at the N-terminus of the HA2 subunit near the envelope. These findings suggest that, for this strain of HA, the structural stability at neutral pH and the exposure of the fusion domain at low pH are influenced by interaction of HA with sialic acid. Further support is provided by the finding that incubation of the virus with sialyl lactose blocks fusion to both ganglioside-containing and ganglioside-free planar membranes. That fusion to sialate-free membranes is inhibited indicates that the binding and fusion domains functionally interact. Supported by NIH grant GM27367.

**Tu-Am-K4**

**Studies on the Mechanism of Inhibition of Fusion by Anti-Viral Peptides.** Daniel R. Kelsey and Philip L. Yeagle, Department of Biochemistry, University at Buffalo School of Medicine (SUNY), Buffalo, New York 14214

The effects of peptides, which inhibit enveloped virus infection and membrane fusion, on the nonlamellar structures formed by N-methyl dioleoylphosphatidyl-ethanolamine (N-methyl DOPE) were studied. The peptides studied, Z-D-Phe-L-PheGly and Z-Gly-L-Phe, were found to partition between the membrane and aqueous phase, slightly favoring the membrane phase due to their relatively hydrophobic structure. Z-D-Phe-L-PheGly, which was an effective inhibitor of viral fusion, broadened the $^{31}P$ nuclear magnetic resonance (NMR) lineshape arising from isotropic nonlamellar structures which have been associated with fusion of N-methyl DOPE large unilamellar vesicles (LUV) in a dose dependent manner. The most significant line broadening occurred in the range of 50 to 100 μM which is also the range where the most effective inhibition of membrane fusion was observed. Z-Gly-L-Phe, which was not effective at inhibiting viral fusion, did not significantly broaden the isotropic $^{31}P$ NMR resonance arising from the N-methyl DOPE LUV in the range of 50 to 100 μM. These data were consistent with an increase in the radius of curvature of the "isotropic" structures in the N-methyl DOPE bilayer. Subsequent studies demonstrated that Z-D-Phe-L-PheGly inhibited the formation of membranes with small radii of curvature. These data collectively suggested a mechanism for inhibition of membrane fusion in which putative fusion intermediates with small radii of curvature were inhibited from forming by the inhibitory peptides. This work was supported by a grant from the NIH (AI 26800).

**Tu-AM-K5**

## FUSION OF INFLUENZA AND SENDAI VIRUSES WITH HUMAN HL-60 AND CEM CELLS.

N. Düzgüneş*#, M. Pedroso de Lima*@, L. Stamatatos*, D. Flasher*, D. S. Friend*, D. Alford*, K. Klappe§, D. Hoekstra§ & S. Nir***. *Univ. of California and #Univ. of the Pacific, San Francisco, @Univ. of Coimbra, Portugal, §Univ. of Groningen, The Netherlands, and **Hebrew Univ., Rehovot, Israel.

The kinetics of fusion of influenza (IFV; A/PR8 strain) and Sendai (HVJ; Z strain) viruses with human promyelocytic leukemia (HL-60) and T lymphocytic leukemia (CEM) cells was investigated. Fusion was demonstrated by electron microscopy, and monitored by fluorescence dequenching of octadecyl rhodamine (R-18) incorporated in the viral membrane. Incubation of IFV with the cells at neutral pH did not cause a significant increase of fluorescence. Rapid and extensive fusion was induced upon mild acidification of the medium. When cells were incubated with IFV pre-treated with proteinase K and the pH reduced, no fluorescence increase was observed, although virus binding to the cells was retained, indicating that the R-18 does not transfer to the target membrane at low pH. The rate constants of adhesion of influenza virus to suspension cells or erythrocyte ghosts, as deduced from binding or fusion experiments, were large, reflecting a diffusion-controlled process. All virus particles could fuse with these cells at pH 5, whereas incomplete fusion activity towards liposomes of mixed phospholipid composition was found previously. The rate constants of fusion of the virus with these cells were several-fold smaller than those found previously for fusion with a variety of liposomes. When IFV was pre-incubated at pH 5 in the absence of target membranes, low pH-induced fusion with erythrocyte ghosts was inhibited, while extensive and rapid fusion with the cultured cells was observed. The kinetic analysis revealed a different mode of low pH-induced inactivation of the virus bound to erythrocyte ghosts or cultured suspension cells.

Sendai virus fused with HL-60 and CEM cells at a slow rate at neutral pH. Fusion was enhanced when the virus was added to the cells at low pH in the case of the Z/G isolate, and inhibited with the Z/SF isolate. Reducing the pH after a short pre-incubation at neutral pH enhanced fusion for both of the isolates. Pre-treatment of the virus at mildly acidic or basic pH did not alter the kinetics of fusion at neutral pH.

Supported by NIH Grant AI-25534, US-Israel Binational Science Foundation Grant 86-00010, and NATO Collaborative Research Grant CRG 900333.

**Tu-AM-K6**

## BINDING OF sCD4 TO HIV-1 AND HIV-1 INFECTED CELLS INDUCES THE RELEASE OF THE ENVELOPE GLYCOPROTEIN GP120.

H. Ellens[1], T. Hart[2], J. Miller[1], R. Kirsh[1], R. Sweet[3] and P. Bugelski[2]. [1]Dept. of Drug Delivery, [2]Dept. of Experimental Pathology, [3]Dept. of Molecular Genetics, SmithKline Beecham Pharmaceuticals, King of Prussia, PA 19406.

HIV (human immunodeficiency virus) introduces its nucleocapsid into the cytoplasm of cells expressing the transmembrane glycoprotein CD4 on their surface. The viral envelope glycoprotein gp120 exhibits high affinity binding to a discrete region within the first domain of CD4. A truncated form of CD4 lacking the transmembrane domain (soluble CD4, sCD4) inhibits HIV infection and HIV-mediated syncytia formation in vitro. It has been assumed that this inhibition results from a competition between sCD4 and cellular CD4 for binding to gp120.We will present evidence that inhibition of HIV-mediated syncytia formation by sCD4 is not simply the result of binding of sCD4 to the gp120/41 complex. Quantitative biochemical and morphological studies show that incubation of HIV-1 infected H9 cells with sCD4 results in removal of gp120 from the surface of infected cells and cell-associated viral particles. This removal of gp120 is dependent on sCD4 concentration (10-1000 nM) and on incubation time (about 50% is released in 20 min.) and temperature (removal does not occur at $4^0$C). Monoclonal anti-CD4 antibodies that inhibit binding of gp120 to CD4 also abolish sCD4 induced removal of gp120. The concentrations of sCD4 needed for removal of gp120 correlate well with those required for inhibition of HIV-mediated syncytia formation. These results suggest that the mechanism of inhibition of syncytia formation by sCD4 is removal of gp120 from the gp120/41 complex. Interestingly, incubation of HIV-1 infected cells with sCD4 at a concentration that induces this removal also results in exposure of a previously cryptic epitope located near the N-terminus of gp41. The N-terminal region of gp41 contains the putative fusogenic sequence. We propose that binding of gp120/41 to cellular CD4 results in a similar removal of gp120, with concomitant exposure of the N-terminal region of gp41, and that this is the first step of the membrane fusion event per se.

**Tu-AM-K7**

## PROPERTIES OF THE PORE FORMED DURING VIRAL HEMAGGLUTININ-MEDIATED FUSION OF AN ERYTHROCYTE TO A FIBROBLAST.

A.E. Spruce, A.Iwata and W.Almers, Dept. Physiology & Biophysics, U. Washington, Seattle, WA.

Fibroblasts (FB) expressing the influenza virus fusion protein (HA) in their plasma membrane (NIH-3T3HA-b2; Doxsey et al, J.Cell Biol. 101:19) were made to fuse to human erythrocytes (RBCs). Fusion is reported by an increase in capacitance (C) of the FB, ultimately by an amount equal to that of a RBC (Spruce et al, Nature 342:555). By analogy to membrane fusion during exocytosis (Spruce et al, Neuron 4:643), the initial fusion pore was characterized by measuring C intermittently; allowing detection of a current transient which flows through the nascent pore (Fig. 1A). The fusion pore conductance (Fig. 1B) is calculated by analysis of the current transient. Similar to the exocytotic fusion pore, the HA-fusion pore opens abruptly. The initial conductance has a median value of 142 pS (range 18-375 pS, n=30). Thereafter, conductance increases more slowly (37 pS/ms, measured from the average of 22 traces). Pore conductance can be followed after the transient is over using the sinusoidal voltage which is used to measure C. Growth of the pore is arrested after its conductance reaches 400-600 pS (within 40 ms). It then fluctuates widely for many seconds (range 4 to > 120 s). Occasionally, subsequent increases occur in steps suggesting additional pore openings. In 3 out of 65 fusions the fusion pore closed and reopened as revealed by return of C to baseline for 10 s or more.

Supported by GM-39520.

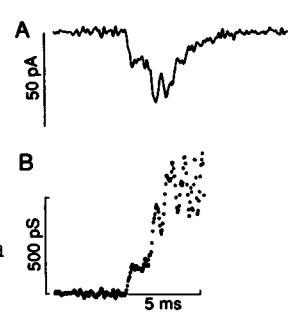


Fig. 1A. Current transient measured at the instant of fusion of a RBC to a FB. B. Fusion pore conductance.

**Tu-AM-K8**

## EVENTS LEADING TO THE OPENING AND CLOSING OF THE EXOCYTOTIC FUSION PORE HAVE MARKEDLY DIFFERENT TEMPERATURE DEPENDENCIES.

A.F. Oberhauser, J.R. Monck and J.M. Fernandez, Dept. of Phys. and Biophys., Mayo Foundation, Rochester, MN 55905.

Exocytosis begins with the formation of a fusion pore, an aqueous channel connecting the lumen of the secretory granule with the extracellular space. The fusion pore typically dilates but frequently closes (flicker). We have been studying the effect of temperature on individual exocytotic fusion and flicker events to gain insight into the chain of events leading to formation and closure of the fusion pore. The fusion of single secretory granules with the plasma membrane was assayed by measuring the cell membrane capacitance. The cells were stimulated by including 10 μM GTPγS in the pipette solution. The rate of formation of the fusion pore ($k_{on}$) was estimated by measuring the mean time between events, Ti; $k_{on}$ = 1/Ti. $k_{on}$ increases exponentially with the temperature, being 0.14 $s^{-1}$ at $6^0$C and 2.9 $s^{-1}$ at $33^0$C. The $Q_{10}$ was 4.7 (between $12^0$C and $24^0$C). This result suggests that the rate limiting steps leading to the formation of the fusion pore are not simple diffusion processes, and involve molecular conformation changes with a high activation energy (30 Kcal/mol). The rate of closure of the fusion pore ($k_{off}$) was estimated by measuring the mean dwell time of the flicker events ($T_f$), and the fraction of flickers per total number of fusion events, Nr; $k_{off} = N_f/T_f$. In contrast to $k_{on}$, $k_{off}$ increases 4-fold between $12^0$C and $14^0$C, whereas above and below this range the $Q_{10}$ was less than 1.8. This coincides with the temperature range at which biological membranes undergo phase transitions. We have previously observed that there is a net transfer of membrane from the plasma membrane to the secretory granule, while they are connected by the fusion pore (Monck et al., 1990, P.N.A.S. 87:7804). The rate of membrane transfer changes 2-fold between $14^0$C and $20^0$C. The temperature dependence of $k_{off}$ and membrane transfer strongly suggest that the fusion pore is partially or completely lipidic during flicker, whereas the temperature dependency of $k_{on}$ suggest a critical role for proteins in the formation of the fusion pore.

**Tu-AM-K9**

TENSION IN SECRETORY GRANULE MEMBRANES CAUSES EXTENSIVE MEMBRANE TRANSFER THROUGH THE EXOCYTOTIC FUSION PORE. Jonathan R. Monck, Andres Oberhauser, Guillermo Alvarez de Toledo, and Julio M. Fernandez. Department of Physiology and Biophysics, Mayo Clinic, Rochester, MN 55905

For membrane fusion to occur the repulsive forces between the two interacting phospholipid bilayers must be reduced. In model systems, this can be achieved by increasing the surface tension of at least one of the membranes using osmotic or hydrostatic forces, electromechanical stress, divalent cations, temperature or membrane "depletion". However, there has so far been no evidence that the secretory granule membrane is under tension. We have been studying guanine nucleotide-stimulated exocytosis in mast cells by measuring plasma membrane area using the patch clamp technique. When a secretory granule fuses with the plasma membrane there is a step increase in the cell surface area. Many of these fusion events are reversible and we have found that for these events the backstep is larger than the initial step indicating that there is a net decrease in the area of the plasma membrane. The decrease has the following properties: (i) the magnitude is strongly dependent upon the life time of the fusion event and can be extensive, representing as much as 40% of the initial granule surface area; (ii) the rate of decrease is independent of granule size; and (iii) the decrease is not dependent upon swelling of the secretory granule matrix. We conclude that the granule membrane is under tension and that this tension causes a net transfer of membrane from the plasma membrane to the secretory granule while they are connected by the fusion pore. The rate of membrane transfer is not dependent on guanine nucleotide concentration (0.2-10 μM) or the osmolarity (80-640 mOs/kg) of the intracellular solutions, and is the same in several phenotypes of mouse in which the mast cell secretory granules have different properties. This suggests that the high membrane tension in the secretory granule may be the critical stress necessary for bringing about exocytotic fusion.

**Tu-AM-L1**

STRUCTURE AND ACTIVITY OF DEGLYCOSYLATED BAND 3, THE ANION TRANSPORT PROTEIN OF THE HUMAN ERYTHROCYTE MEMBRANE. Reinhart A.F. Reithmeier, Joseph R. Casey and Charles A. Pirraglia, MRC Group in Membrane Biology, Department of Medicine and Department of Biochemistry, University of Toronto, Toronto, Ontario, Canada, M5S 1A8.

The effect of enzymatic deglycosylation on the structure and transport activity of Band 3, the anion transport protein of the human erythrocyte membrane was determined. N-linked carbohydrate could be removed from Band 3 in 0.1% octaethylene glycol mono n-dodecyl ether ($C_{12}E_8$) detergent solution by glycopeptidase F treatment, as shown by a shift in mobility of the protein during sodium dodecyl sulfate gel electrophoresis and by loss of tomato lectin binding. The deglycosylated protein maintained its oligomeric structure but had a slightly smaller Stokes radius than native Band 3 as determined by size exclusion HPLC. The maximal amount of $C_{12}E_8$ bound by Band 3 (0.6 mg detergent/mg protein) was unaffected by deglycosylation. Circular dichroism studies showed that deglycosylation did not change the secondary structure of the protein. The sensitivity of the purified protein to proteolytic digestion by proteinase K was increased slightly by deglycosylation and the deglycosylated protein was more readily precipitated by ammonium sulfate. The deglycosylated protein bound the transport inhibitor 4-benzamido-4'-amino-2,2'-stilbene disulfonate with the same affinity (Kd = 1 μM) as the native protein. Transport studies using resealed ghosts that had been treated with glycopeptidase F showed that deglycosylation of Band 3 had no effect on its ability to transport anions or on the sensitivity of transport to inhibition by stilbene disulfonates. (Supported by the Medical Research Council of Canada).

**Tu-AM-L2**

**IRREVERSIBLY ACTING INHIBITORS OF BAND 3 PROTEIN-MEDIATED ANION TRANSPORT STUDIED AFTER EXPRESSION OF MOUSE BAND 3-ENCODING cRNA IN XENOPUS OOCYTES** D. Kietz, D. Bartel, S. Lepke, H. Passow; intro. by S. Dissing. Max-Planck-Inst. of Biophysics, Frankfurt/M., FRG

Wild type band 3 and band 3 mutated at lys 558 or lys 608 or both were expressed and inhibition by $H_2$DIDS, 1-fluoro-2,4-dinitrobenzene (DNFB) and phenylisothiocyanate (PITC) of $Cl^-$ efflux from single oocytes was studied. After fast reversible binding, $H_2$DIDS inhibits with $K_{0.5}$ = 0.3 μM. Subsequent slow covalent bond formation follows first order kinetics. pH dependence of reaction rate yields pK values for wild type and mutant (asn 558) that differ by 2 pK units and are indistinguishable from those of two lys residues involved in intramolecular cross-linking of band 3 by $H_2$DIDS in red cells. Unlike $H_2$DIDS, neither DNFB nor PITC produce noncovalent inhibition. Hence covalent reaction takes place while $Cl^-$ efflux proceeds. Decrease of $^{36}Cl^-$ inside an oocyte (y) as function of time (t) and inhibitor concentration [i] should follow the equation: $\ln y/y_0 = -k_a/k_b\,(1-\varphi)(1-\exp(-k_b[i]t)) - \varphi\, k_a\, t$ where $k_a$ = rate constant of band 3-mediated efflux at zero inhibition, $\varphi$ = fraction of $k_a$ persisting after reaction of all band 3 molecules with i, $k_b$ = rate constant for reaction of i with band 3 protein. In the mutant asn 558, $k_b$ for DNFB is reduced by 80% as compared to wild type, suggesting that lys 558 is more susceptible to react with amino group reagents than other transport-related lysines. The slower inhibition after mutation of lys 558 indicates the reaction of DNFB with additional, less reactive groups the significance of which cannot be recognized in the wild type where the high reactivity of lys 558 hides their influence. The PITC shows more complex behavior, and results with red cells and oocytes are not easily reconciliable.

**Tu-AM-L3**

A CYTOPLASMIC PROTEIN INVOLVED IN CALCIUM-ACTIVATED POTASSIUM TRANSPORT CAN SERVE AS A SUBSTRATE FOR CYCLIC GMP-DEPENDENT KINASE. G.A. Plishker *, S.K. Shriver**, and D.L. Chevalier*, R.B. Moore**. *Department of Neurology, Baylor College of Medicine, Houston TX, and **Departments of Pediatrics and Biochemistry, University of South Alabama, College of Medicine, Mobile AL.

Calpromotin, a cytoplasmic protein that is involved in the regulation of Ca-activated potassium transport in red blood cells, is a specific substrate for cyclic GMP-dependent kinase. The calcium-dependent membrane association, as well as the carboxymethylation of calpromotin, correlate with the loss of potassium from red blood cells (Plishker, AJP 248:C419-C424, 1985). Calpromotin alone is required to reconstitute Ca-activated K transport in red cell membrane vesicles (Moore et al., Blood 72:32A, 1988). Purified calpromotin is a highly specific substrate for cGMP-dependent kinase purified from bovine lung. When calpromotin is in excess the phosphorylation is proportional to the kinase concentration. Phosphorylation of calpromotin by cAMP-dependent kinase is 100 fold less effective. Both kinases were very effective in phosphorylating histones. Calmodulin-dependent kinase and protein kinase C did not phosphorylate calpromotin. Immunological screening indicates that calpromotin is present in adrenal glands, brain, and lung, with lower levels in in spleen, smooth muscle, skeletal muscle, liver, kidney and platelets. In dissociated cultures prepared from cerebral cortices of rat embryos, calpromotin is localized to neurons. The amount of calpromotin in extracts from embryonic rat cerebral cortices increases from 6.98 ug/mg protein for 12 day embryos, to 27.55 ug/mg protein for 16 day embryos. Initially, the protein is localized to the soma, but by the 16th day it extends into the branched processes of the cell. Supported by grants from NIH.

**Tu-AM-L4**

INHIBITION OF THE HUMAN RED CELL CA-ATPASE BY CYTOPLASMIC FACTORS

G. Wang, V. Barrett, J. Ye-Hu, D.R. Yingst

Department of Physiology, Wayne State School of Medicine, Detroit, MI

The inhibitory effect of human red cell hemolysate on the Ca-ATPase (Sheikhnejad, R.G., et al., 1987. J. Gen. Phys. 90:37a) is, in part, due to a factor(s) with a molecular weight between 500 and 1,000 daltons. This estimate is based on the observation that some of the active fractions passed through a YM2 filter with a 1,000 MW cutoff (Amicon Div., Danvers, MA, USA), but were subsequently retained on top of a YC05 (Amicon) filter with a 500 MW cutoff. Samples applied to the YM2 filter were isolated from the hemolysate of human red blood cells by Ca-dependent hydrophobic interaction and anion exchange chromatography followed by filtration through a PM10 membrane (Amicon), which has a 10,000 MW cutoff. The sample that was retained on the YC05 filter inhibited the Ca-ATPase of the human red cell membrane in a dose-dependent manner when assayed at a constant value of 2 uM free Ca. YC05 samples, however, also chelated Ca, which caused additional inhibition of the Ca-ATPase when the free Ca was not held constant. To assure that the level of free Ca in the assay was the same in the presence and absence of the YC05 sample, we monitored the final free Ca in the Ca-ATPase assays by means of arsenazo III, a Ca-sensitive dye. It is not yet known if the factor (calcatin) that inhibited the Ca-ATPase at constant free Ca is the same as the chelator. YC05 samples contained a silver-staining band of 600 to 1,000 daltons (90% pure), as analyzed by SDS PAGE fractions under reducing conditions. This band was present in the assays at sufficient concentrations to account for the inhibition of the Ca-ATPase at constant free Ca. It was present, however, at too low a concentration to explain the observed chelation. (Supported by a grant from the Cystic Fibrosis Foundation and by the National Science Foundation.)

Tu-AM-L5

**RBC MEMBRANE AREA AND VOLUME REGULATION DURING NON-ISOTONIC PERFUSION**

Engström KG, Möller Bţ, and Meiselman HJ. Dept of Physiology and Biophysics, University of Southern California, School of Medicine, Los Angeles, CA 90033, USA, and Carl Zeiss, Oberkochen, West Germanyţ.

In order to directly examine the dynamic response of human red blood cell (RBC) volume and membrane surface area to non-isotonic media, we studied unfractionated RBC partially aspirated into glass micropipettes. These studies employed a new perfusion chamber (Estra250, Carl Zeiss, Sweden) which allows rapid changes (≈500ms) of media, and video recording/digital image analysis for detailed temporal information. In order to eliminate optical artifacts associated with pipette measurements, the following factors were considered:
1) Pipette Internal Diameter (PID). Since the pipette functions as a one-plane spherical lens, the apparent PID is an overestimate closely proportional to the glass/liquid refractive index ratio (1.52/1.33 =1.143). This problem was confirmed by studying pipettes bent to permit observations of the horizontal (H) and vertical (V) projections of PID; for paired measurements the H/V ratio was 1.12±0.01 (±SEM) and thus in agreement with the refractive index ratio.
2) Pipette Internal Cone Angle (PICA). The PICA was found to vary with the pulling procedure (mean value of 1.4±0.08°) and to markedly influence the calculated RBC geometry.
3) Diffraction Phenomenon. Due to diffraction, the apparent RBC size is overestimated. Using opposing pipettes with two aspirated RBC, the true RBC contour was found to be 0.09 μm from the outer edge of the diffraction band and to also affect the calculated RBC geometry.

Using these corrections and exact mathematical equations, our data at 200 mOsm indicate an initial peak increase of both volume (39±1.2%) and surface area (7.0±0.4%) at about 8-9s of perfusion, following which these parameters decreased over a 5 min period to 30±0.8% and 3.7±0.8%. These unexpected changes in area were even larger without the optical corrections and cannot be explained due to a RBC spherical shape and/or excessive membrane tension (*i.e.*, 1.9μm PID, -20mm $H_2O$, tension= 0.17 dyn/cm). Qualitatively similar results were obtained at 130 mOsm, with inverse changes observed at 400 mOsm. In overview, our findings indicate that RBC surface area, as well as volume, are regulated under non-isotonic conditions and thus suggest a sensitivity of the RBC cytoskeleton to anisotonic media.
Supported by MFR(12x-2288), HL15722, and HL41341.

Tu-AM-L6

**THE RELATIONSHIP BETWEEN SPECTRIN STRUCTURE AND RED CELL SIZE** Li Li, Amy McGough, and Robert Josephs, Dept. of Molecular Genetics and Cell Biology, University of Chicago, Chicago, IL 60637

We have carried out a three dimensional reconstruction of spectrin using electron micrographs such as those in figures 1 and 2 in McGough and Josephs (*PNAS* **87** 5208 - 5212 [1990]). The axial view of the reconstruction shows the subunits are elliptical with major and minor axes of 30 Å and 18 Å respectively. The lateral view shows the helical twist of the subunits. A similar helical twist can be seen in micrographs of spectrin (for instance in figure 2 of McGough and Josephs) although the high noise level partially obscures their clarity. The results of the reconstruction support the model proposed for spectrin in McGough and Josephs.

Red cells in physiological saline are 8 μ in diameter. Given the number of spectrin molecules in a red cell ($10^5$), the area of a red cell (135 $\mu^2$), and that the array is approximately hexagonal one can readily calculate that average length of a spectrin molecule is 700 - 750Å (Steck, T. L. *J. Cell Biol* **62** 1-19[1974]). The diameter of isolated skeletons depends upon the ionic strength of the solution because of variations in the length of the component spectrin molecules. We have measured the skeleton diameter for skeletons suspended in solutions at different ionic strengths. At high ionic strengths the diameter of the skeleton reaches a limiting size of 3.5 μ which corresponds to a spectrin molecule that is 370 Å long. We now consider how our proposed model for the structure of the spectrin molecule accounts for this limiting size.

The preliminary three dimensional reconstruction of spectrin permits an estimate of the shortest length a spectrin molecule can attain subject to the constraints that (1) the molecule maintains the helical structure proposed by McGough and Josephs and (2) the α and β subunits **do not interpenetrate**. The shortest possible pitch occurs when successive turns of the helix just touch since a shorter pitch would result in interpenetration of the subunits. Given this constraint the shortest possible pitch is 36 Å. This in turn leads to a molecular length of 360 Å since the molecular helix makes ten turns. Thus the structural data (reconstructions of the EM data and modeling) provide a physical basis for the solution behavior of spectrin in intact skeletons and both sets of data point to a limiting length of 360 - 380 Å for the spectrin molecule in intact skeletons.

Tu-AM-L7

EVIDENCE THAT SPECTRIN RESTRAINS THE EXPANSION OF A FUSION ZONE IF IT IS CREATED BETWEEN TWO ERYTHROCYTE GHOSTS IN CONTACT AND EVEN IF THE SPECTRIN IS INTACT IN ONLY ONE OF THE TWO GHOST MEMBRANES. L.V. Chernomordik* and Arthur E. Sowers, Cell Biology, ARC/Holland Laboratory, Rockville, MD 20855.

Cell + Cell fusions are often accompanied by a morphological change in which two spherical cells in contact develop an hour-glass constriction (or lumen) which expands in diameter until the morphological change ends in a single sphere with a larger diameter (="giant cell"). Electrofused erythrocyte ghosts held in contact by peal chain formation with dielectrophoresis revealed that the lumen diameter increase did not permit giant cell formation unless the ghosts were heated above the spectrin denaturation temperature. The sub-maximal lumen diameters in the linear chains of fused ghosts were stable for up to 3 days at 0-4℃. The hypothesis that spectrin itself was responsible for restraining the lumen expansion was successfully tested by both low ionic strength and low pH treatments, also known to alter the spectrin network. Collection of the stable linear chains of fused erythrocyte ghosts and processing for thin section electron microscopy showed that each stable lumen bordering two adjacent fused ghosts was composed of a "perforated septum" composed of two close-spaced membranes interrupted at regular intervals by fusion sites. The perforated septum -- actually a fusion zone -- is thus a stable post-fusion product. Using DiI as a membrane label to follow fusions between heat-treated and non heat-treated ghosts, it was found that if only one of the two ghosts had an intact spectrin network, the fusion lumen was still prevented from expanding to the giant sphere morphology. The use of osmoticants external to the ghost membranes indicated that osmotic pressure differences were not responsible for the forces which cause giant cell formation (i.e. when there is no restraint from heat-released spectrin). *Permanent address: A.N. Frumkin Institute, Acad. Sci. USSR, Moscow. Supported by ONR grant N00014-89-J-1715 to AES.

Tu-AM-L8

**DDAVP INDUCES ADHESION OF SICKLE RED CELLS WITHOUT CAUSING OBSTRUCTION: MRI AND TEM STUDIES.** M E Fabry, S M Suzuka, R L Nagel, and D K Kaul, Department of Medicine, Albert Einstein College of Medicine, Bronx, NY.

The densest red cells have been found to selectively disappear from the circulation of sickle cell anemia patients (SS) during painful crisis which led to the proposal that dense cell (SS4) trapping at the site of vaso-occlusion is the most likely explanation for pain and ischemia observed. More recently Tsai et al (Tsai, Sussman, Nagel, and Kaul Blood 73s:116a, 1988) demonstrated that adhesion of SS discocytes (SS2) to post-capillary venules in the isolated rat mesocecum is DDAVP-stimulated, von Willebrand factor (vWF)-mediated. Using an intact animal model which involves injecting saline-washed, density-defined SS red cells into the femoral artery of a rat, we have explored the potential of DDAVP to stimulate adhesion in vivo. SS2 and SS4 cells were isolated by density gradient centrifugation and injected into the femoral artery 15 minutes after exposure to 0.4 μg/kg DDAVP (which stimulates release of vWF). Quantitative studies of the number of red cells retained in the rat thigh using $^{99m}$Tc-labelled red cells and gamma camera imaging demonstrated that DDAVP increases retention of AA cells from 0.54 to 1.43 μl cells/leg ($p<0.0005$), while that of SS2 cells was increased from 4.4 to 12.2 μl cells/leg ($p<0.026$), and that of SS4 cells from 12.7 to 15.9 μl cells/leg ($p<0.22$)($N = 4, 5, 4, 18, 33, 11$ respectively). Measurement of tissue water proton relaxation time in the thigh by H-1 MRI (magnetic resonance imaging) revealed that retention of SS4 cells induced a dose dependent increase in tissue edema while retention of AA or SS2 cells produced no change. The cause of this difference in behavior was examined by transmission electron microscopy. After injection of cells via femoral artery cannulation, the thigh was first flushed with isotonic saline and then with glutaraldehyde and sectioned. We observed that both AA and SS2 cells (all SS cells were identifiable by polymer formation) could be observed adhering to the walls of vessels of moderate size which had clear lumens indicating that free passage of both cells and plasma were possible. In constrast, SS4 cells were observed in obstructed vessels with trapped plasma and rat red cells. We hypothesize that adhesion of SS2 cells could narrow the lumen of post-capillary venules thereby promoting trapping of SS4 cells which then leads to vaso-occlusion.

**Tu-AM-L9**

**ACTION OF PLATELET-ACTIVATING FACTOR ON ERYTHROCYTE MEMBRANE.**

A. Kantar, P.L. Giorgi, G. Curatola*, R. Fiorini*
Depts. of Pediatrics and Biochemistry*, University of Ancona, via Corridoni 11, Ancona 60123, Italy.

1-O-alkyl-2-acetyl-sn-glycero-3-phosphocholine, PAF, is a naturally occurring phospholipid released from various cell types. It exhibits a broad range of biological activities in a variety of cells. Recently, we reported an effect of PAF on the physico-chemical organization of erythrocyte membranes using fluorescence spectroscopy and 1-(4-trimethyl ammoniumphenyl)-1,3,5-hexatriene (TMA-DPH) as fluorescent probe. Low concentration of PAF ($10^{-7}$ M) induced a time-limited decrease of TMA-DPH steady-state fluorescence anisotropy, and a decrease of erythrocyte membrane microheterogeneity (1).

In this study hemoglobin-free erythrocyte membranes have been incubated with PAF ($10^{-7}$M) and consequently lipids were extracted from membranes at different times of incubation. Lipid extracts were analyzed for detecting the formation of conjugated diene hydroperoxides by measuring the absorbance ratio $A_{233\ nm}$ / $A_{215\ nm}$, defined as the "oxidation index". Our results demonstrated a significant increase of hydroperoxides in PAF treated erythrocyte membranes.

(1) A. Kantar, P.L. Giorgi, G. Curatola, R. Fiorini : Effect of PAF on erythrocyte membrane heterogeneity: A fluorescence study. Agents and Actions ( in press ).